



Review

Effect of Hot Deformation and Heat Treatment on the Microstructure and Properties of Spray-Formed Al-Zn-Mg-Cu Alloys

Lingfei Cao ^{1,2}, Xiaomin Lin ¹, Zhenghao Zhang ¹, Min Bai ¹ and Xiaodong Wu ^{1,*}

¹ International Joint Laboratory for Light Alloys (Ministry of Education), College of Materials Science and Engineering, Chongqing University, Chongqing 400044, China; caolingfei@cqu.edu.cn (L.C.); linxm@cqu.edu.cn (X.L.); zhangzhenghao@stu.cqu.edu.cn (Z.Z.); baimin@stu.cqu.edu.cn (M.B.)

² Shenyang National Laboratory for Materials Science, Chongqing University, Chongqing 400044, China

* Correspondence: xiaodongwu@cqu.edu.cn

Abstract: Spray forming is a manufacturing process that enables the production of high-performance metallic materials with exceptional properties. Due to its rapid solidification nature, spray forming can produce materials that exhibit fine, uniform, and equiaxed microstructures, with low micro-segregation, high solubility, and excellent workability. Al-Zn-Mg-Cu alloys have been widely used in the aerospace field due to their excellent properties, i.e., high strength, low density, and outstanding machinability. The alloy manufactured by spray forming has a combination of better impact properties and higher specific strength, due to its higher cooling rate, higher solute concentration, and lower segregation. In this manuscript, the recent development of spray-formed Al-Zn-Mg-Cu alloys is briefly reviewed. The influence of hot working, i.e., hot extrusion, hot forging, and hot rolling, as well as different heat treatments on the property and microstructure of spray-formed Al-Zn-Mg-Cu alloys is introduced. The second phases and their influence on the microstructure and mechanical properties are summarized. Finally, the potential in high-temperature applications and future prospects of spray-formed aluminum alloys are discussed.

Keywords: Al-Zn-Mg-Cu alloys; spray forming; hot deformation; heat treatment; precipitation



Citation: Cao, L.; Lin, X.; Zhang, Z.; Bai, M.; Wu, X. Effect of Hot Deformation and Heat Treatment on the Microstructure and Properties of Spray-Formed Al-Zn-Mg-Cu Alloys. *Metals* **2024**, *14*, 451. <https://doi.org/10.3390/met14040451>

Academic Editor: Maciej Motyka

Received: 6 March 2024

Revised: 4 April 2024

Accepted: 8 April 2024

Published: 11 April 2024



Copyright: © 2024 by the authors. Licensee MDPI, Basel, Switzerland. This article is an open access article distributed under the terms and conditions of the Creative Commons Attribution (CC BY) license (<https://creativecommons.org/licenses/by/4.0/>).

1. Introduction

Al-Zn-Mg-Cu alloys, characterized by low density and high specific strength, are widely applied in the aerospace industry, high-speed trains, and various other engineering fields. To further enhance the overall performance of this series of alloys, extensive investigations have been conducted [1–5], including modifications to the chemical composition and the adoption of new production methods. Consequently, spray forming, a technique that has demonstrated clear advantages in producing ingots with fine grains, a uniform structure, and minimal oxidation, was introduced to fabricate high-alloying and high-strength aluminum alloys [6,7]. Over the recent decades, spray-formed Al-Zn-Mg-Cu alloys have undergone successful development and have been progressively commercialized [8–10]. To attain a better understanding of these alloys, an overview of their development history, associated hot deformation behavior, heat treatment, and precipitation behavior is provided in this paper. A strategy for applications at elevated temperatures is proposed, and future development directions for these alloys are envisioned.

2. Development of Spray-Formed Al-Zn-Mg-Cu Alloy

Spray forming, also referred to as spray deposition or spray casting, is identified as a near-net shape technique that has been developed from rapid solidification/powder metallurgy [11–14]. In this process, the spray atomization stage and the spray deposition stage are incorporated. The process is shown in Figure 1. Under the protection of inert gases (typically He, Ar, or N₂), alloy melt flows out through the delivery tube by its own gravity (tight coupling type), or falls freely from the bottom of the crucible directly by its

own gravity (free falling type) to the atomization zone formed by the gas ejected from the nozzle. In the atomization zone, high-pressure gas atomizes the alloy melt into fine liquid droplets and sprays them onto the deposition plate; the droplets rapidly cool during flight (up to 10^3 – 10^7 Ks⁻¹) [15], finally landing on the deposition plate in a semi-solidified state, where the semi-solidified liquid droplets aggregate together, continue to cool, and eventually solidify to form the deposited blank. Materials produced by this process exhibit fine, uniform, and equiaxed microstructures, with low micro-segregation, high solubility, and excellent workability, which result from the fine and uniform microstructures [16–22]. While in traditional casting processes, different cooling conditions of the casting mold lead to different morphologies of the ingot structure. The macrostructure of the ingot usually consists of three crystal zones: a fine crystal zone on the outer surface, a columnar crystal zone in the middle, and an equiaxed crystal zone in the core. The ingot structure may also exhibit defects such as porosity and shrinkage, which have adverse effects on the alloy properties [23]. Due to the differences in the solidification process of the alloy melt between spray-forming and traditional casting processes, materials prepared by these two methods show significant disparities in microstructural morphology. Compared with ingots produced by conventional casting, those obtained from spray forming are noted to eliminate or minimize segregation, as demonstrated in Figure 2, due to the cooling rate being as high as 10^3 – 10^7 Ks⁻¹ [15]. By the late 1980s, spray forming had begun to be commercialized [24], and currently, many institutions and companies are actively engaged in this field, including Sandvik Osprey Ltd., Sandviken, Sweden, Sumitomo Heavy Industries Ltd., Tokyo, Japan, Baoshan Iron & Steel Co., Ltd., Shanghai, China, Heye Special Steel Co., Ltd., Shijiazhuang, Hebei, China, and Jiangsu Haoran Spray Forming Alloy Co., Ltd., Zhenjiang, China.

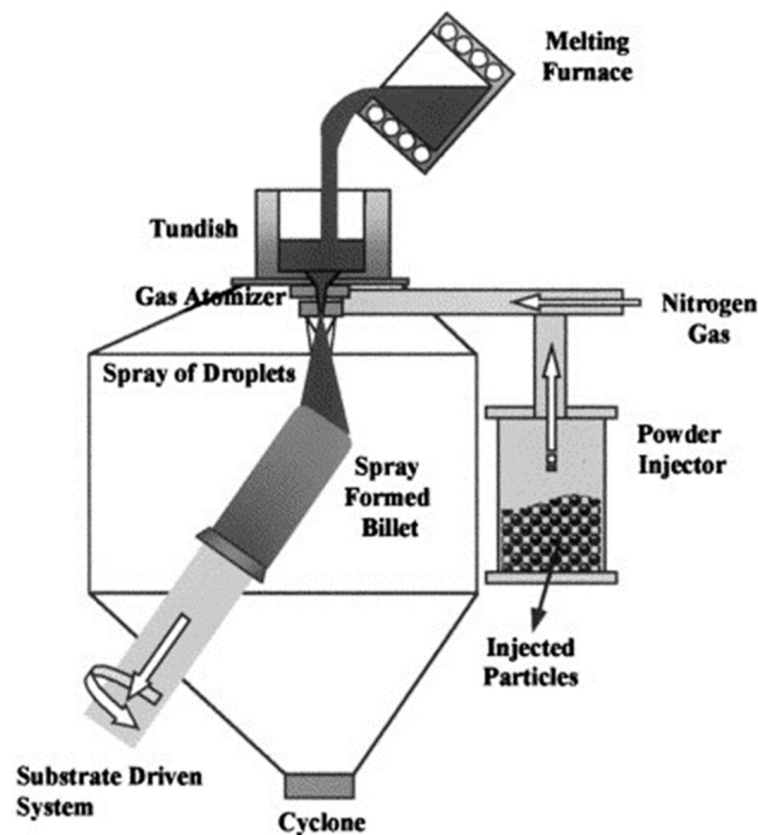


Figure 1. A schematic diagram of the spray-forming equipment used in the present study [25].

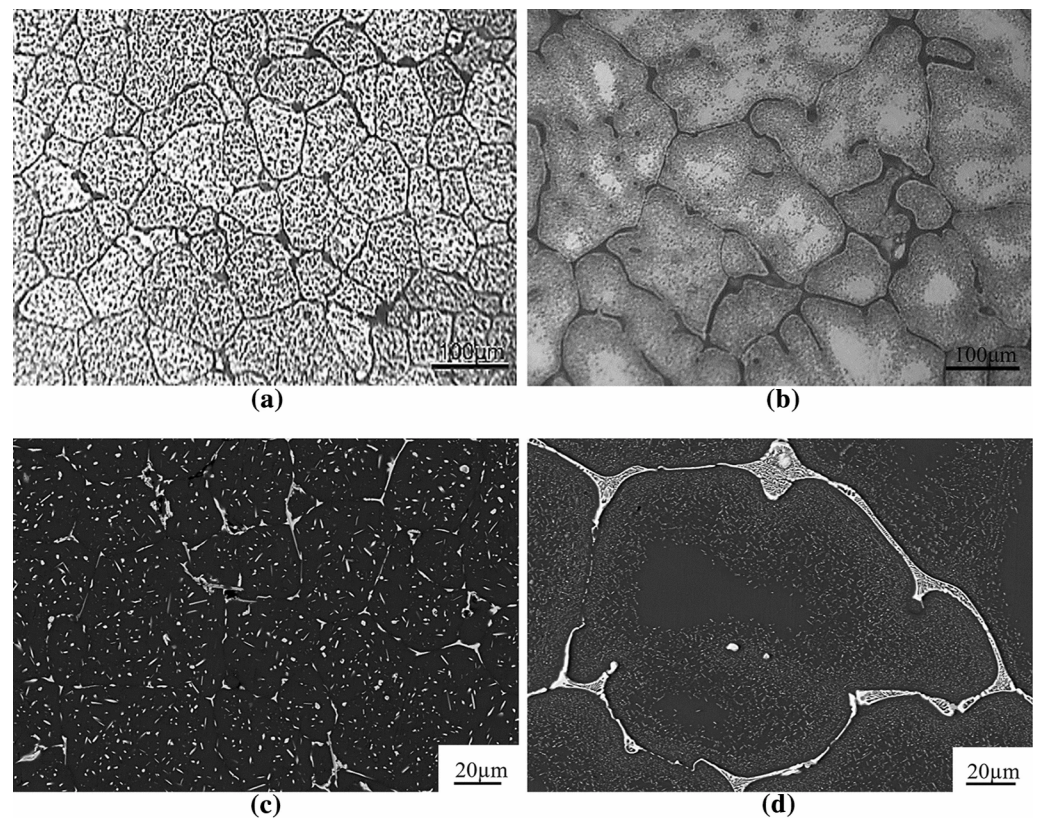
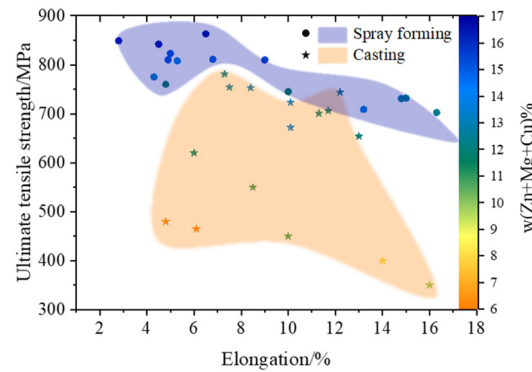


Figure 2. Typical optical images and backscattered SEM BSE micrographs of 7055 alloy ingots: (a,c) as deposited and (b,d) as cast [9].

Over the past decades, considerable attention has been given to improving the strength level of Al-Zn-Mg-Cu alloys through spray forming [26–29]. In 1998, Osprey Metals Ltd. (Sandviken, Sweden) achieved the mass production of spray-formed 7034, containing up to 11.5 wt.% Zn. After aging, the tensile strength of this alloy at room temperature reached up to 800 MPa, and the elongation was above 8%, marking a significant improvement over traditional casting products. Presently, this alloy is applied in the manufacture of structural components, including connecting rod and shaft support seats for high-speed racing engines [30]. Concurrently, spray-formed 7093 was developed at the University of Pennsylvania with a Zn content of approximately 9.5 wt.%, achieving a tensile strength at room temperature of up to 760 MPa and an elongation of 11% [31]. Ultimate tensile strength and elongation at peak aging for spray-formed Al-Zn-Mg-Cu alloys are listed in Table 1, which provides valid evidence for the fact that the spray-formed alloys have superior strength. In China, research on spray forming was initiated in the early 1990s [32], with entities such as Central South University, General Research Institute for Nonferrous Metals, and Jiangsu Haoran Spray Forming Company actively participating in this field. High-performance alloys such as 7034, 7050, 7075, and 7055 have been successfully fabricated by spray forming. For instance, spray-formed 7055, featuring a more uniform composition and second-phase distribution, can achieve a fracture toughness of $30.7 \text{ MPa}\cdot\text{m}^{1/2}$ in the L-T direction, potentially replacing 2A14 in helicopter hub applications to enhance stability and safety [33]. Obvious advantages are presented by spray forming in the production of highly alloyed Al-Zn-Mg-Cu alloys, with the ultimate tensile strength of heat-treated Al-11.3Zn-2.4Mg-1.1Cu alloys reaching 796 MPa [34]. To date, spray forming has been recognized as one of the best methods for preparing Al-Zn-Mg-Cu alloys, due to the significant improvement in their mechanical properties compared to those of cast alloys, as shown in Figure 3.

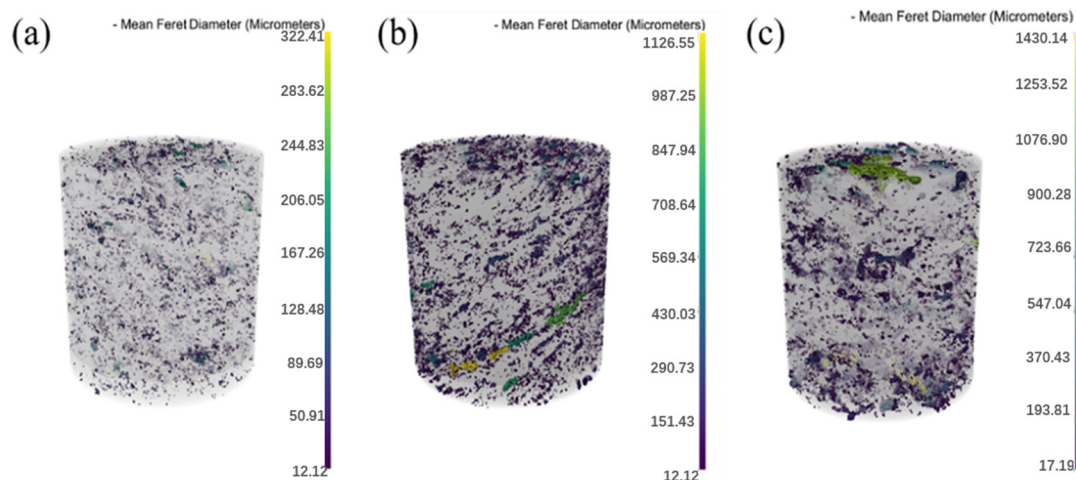
Table 1. Mechanical properties of spray-formed Al-Zn-Mg-Cu alloys at peak aging [35–40].

Alloy Composition (wt%)				Ultimate Tensile Strength (MPa)	Elongation (%)
Zn	Mg	Cu	Zr		
11~12	2~3	0.8~1.2	-	808	5.29
10.78	2.45	1.7	-	811	6.8
8.15	1.97	2.46	-	731	14.8
11.38	11.38	2.45	1.1	878.6	5.60
11.3	11.3	2.65	1.06	823	5
6.52	2.53	2.39	0.12	745	10

**Figure 3.** Mechanical properties of peak aged Al-Zn-Mg-Cu alloys prepared by spray forming and conventional ingot metallurgy (casting) [26,27,35–50].

3. Hot Deformation of Spray-Formed Al-Zn-Mg-Cu Alloys

During the spray-forming process, droplets of Al-Zn-Mg-Cu alloys are subjected to rapid cooling from high temperature to room temperature, resulting in potentially different solidification outcomes for each droplet. In that case, 1–10% of pores may appear in the deposited billet [51], which is not desirable for its direct application [52]. An overview is provided in Figure 4 of pores detected by a 3D X-ray microscope at different positions within the ingot. It is evident that a high density of pores is observed in the as-deposited alloy, and the pore size varies at different positions; the edge of the billet exhibits larger pores than the center region [53]. To achieve a more uniform microstructure and superior performance, densification and further deformation are typically achieved through methods such as hot extrusion, forging, and rolling [54–59].

**Figure 4.** 3D perspective of pores in the as-deposited alloy: (a) center, (b) half the radius, and (c) edge of the billet [53].

3.1. Hot Extrusion

Hot extrusion is commonly utilized to process the spray-formed billets. During this process, the billet is subjected to triaxial compressive stress and shear forces due to mutual friction with the mold and varying speeds of the components [60]. As shown in Figure 5, these combined effects lead to the compaction of pores within the billet without initiating cracks, resulting in improved plastic deformation during hot extrusion and ultimately a relative density of more than 98% [61–63]. Jia et al. [53] discovered that hot extrusion significantly enhances the mechanical properties of spray-formed 7055. After a 25:1 hot extrusion treatment, the strength of the alloy increased from 120 MPa to over 330 MPa, and the elongation increased from less than 1% to more than 9.5%, due to the elimination of micropores and a more homogeneous distribution of the second phases which are crushed during the extrusion process. The significant parameters of extrusion process that influence the densification and microstructure of spray-formed billets are the extrusion ratio and temperature. Furthermore, the extrusion temperature impacts work hardening, dynamic recovery, and dynamic recrystallization processes, thereby affecting the final performance of the alloy.

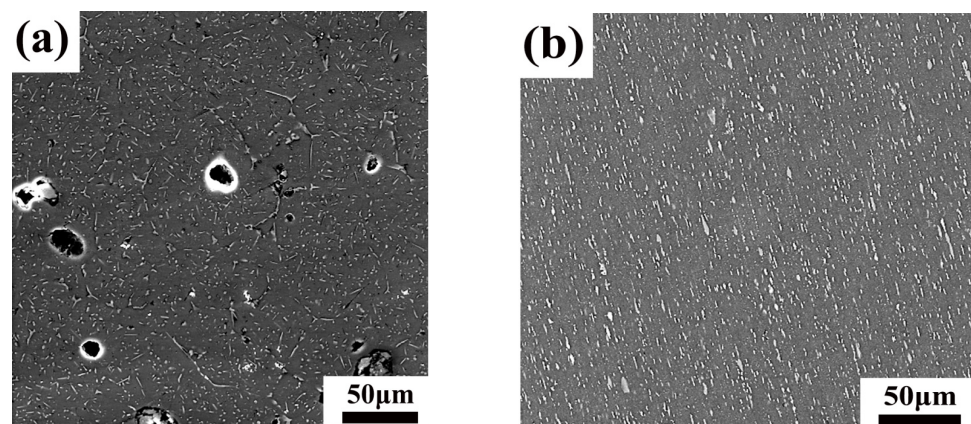


Figure 5. SEM photographs of spray-formed 7055 AA following extrusion showing microstructure (a) as deposited and (b) as hot extruded.

At different extrusion temperatures, the recrystallization behavior and mechanical properties vary significantly during deformation, with a typical extrusion temperature range of 350–500 °C for Al-Zn-Mg-Cu alloys [64]. Wang et al. [65] designed a two-step extrusion process for industrial-scale spray-formed 7055 alloy. An extrusion ratio of 3.84:1 is applied in the first step to weld pores and achieve uniform structure, leading to a tensile strength of 347 MPa. The second step employed an extrusion ratio of 8.65:1, finally increasing the alloy's tensile strength to 382 MPa. Wei et al. [66] studied the hot extrusion process of spray-formed Al-Zn-Mg-Cu alloys, extrusion ratios of 7:1, 14:1, and 28:1 are used for the densification of deposited billets. The results showed that all three extrusion ratios could eliminate micro-porosity and achieve a relatively dense structure. However, the as-extruded alloy's performance varied depending on the amount of deformation, such as the tensile strength being 250 MPa at an extrusion ratio of 7:1, and increasing to 372 MPa at an extrusion ratio of 28:1. Consequently, suitable extrusion ratios ought to be selected in the actual production process, based on the characteristics of different alloys and their intended applications.

3.2. Forging

Pressure is applied to alloys through forging to induce plastic deformation, resulting in the production of forged components with specific shapes, dimensions, and properties. As shown in Figure 6, in the case of spray-formed alloys, porosity is commonly eliminated, defects are reduced, and grains are further refined through hot forging, thereby enhancing strength. Multidirectional forging at 350 °C was employed by Kishchik et al. [67] to reduce

pore size in the spray-formed Al-4.8Mg-1.2Mn-0.1Cr alloy and to form an equiaxed grain structure with grain sizes of approximately 6 μm in the recrystallized sheet. The effects of square cladding forging on the density and mechanical properties of spray-formed Al-8.5Zn-3.4Cu-1.7Mg alloy were studied by Xu et al. [68]. Following square cladding forging, it was found that the alloy's density exceeded 99%, with the ultimate tensile strength and elongation increasing from 285 MPa and 4.6% in the as-deposited state to 397 MPa and 6.1%, respectively. Subsequent to T6 heat treatment, the ultimate tensile strength was further increased to 607 MPa, whereas the elongation slightly decreased to 5.2%. Furthermore, forging combined with extrusion (at a ratio of 24:1) was utilized by Khan et al. [57] on the spray-formed 7055 alloy, resulting in the refined microstructures shown in Figure 6. The alloy's tensile strength increased from 224 MPa in the as-deposited state to 415 MPa in the hot deformation state, and finally reached 784 MPa in the T6 state.

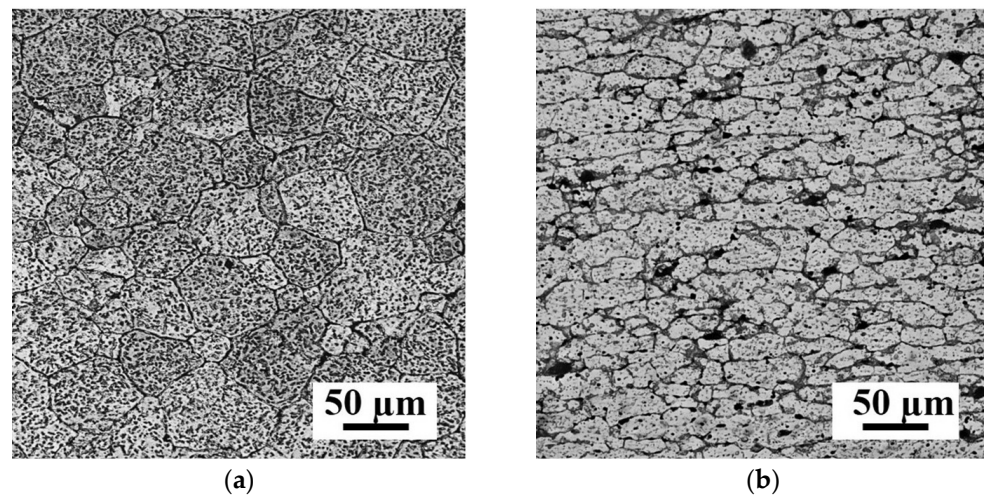


Figure 6. Microstructure of the Al-Zn-Cu-Mg alloy processed by (a) spray forming and (b) spray forming followed by hot forming processes (hot forging and hot extrusion) [57].

3.3. Rolling

Rolling is identified as a key technology in forming Al-Zn-Mg-Cu alloy sheets. Through interaction with the rolls, the billet undergoes plastic deformation [69]. The microstructural comparison between the as-deposited and hot-rolled spray-formed alloy is illustrated in Figure 7. The applied pressure during the rolling process refines or even eliminates pores within the billet, resulting in the material's densification. Moreover, grains are refined and coarse second phases are crushed post-rolling, significantly enhancing the mechanical properties [70]. Currently, conventional symmetric rolling and asymmetric rolling are the processes predominantly utilized in industrial production [71,72]. The effectiveness of rolling is primarily influenced by the rolling temperature and rolling speed. Selecting suitable rolling parameters allows for the control of grain growth and precipitation behavior. The impact of various rolling temperatures on the rolling effectiveness and alloy properties has been thoroughly investigated. Mei et al. [73] discovered that a warm rolling process at 120 $^{\circ}\text{C}$ results in a more uniform distribution of solute atoms and vacancies in an Al-7.7Zn-2.2Mg-2.0Cu alloy, consequently leading to a more consistent precipitation distribution during aging. Additionally, Xiang et al. [36] conducted homogenization (at 350 $^{\circ}\text{C}$ for 5 h followed by 470 $^{\circ}\text{C}$ for 24 h with a heating rate of 30 $^{\circ}\text{C}/\text{h}$ from room temperature) on the 7034 alloy, then performed warm rolling at 200 $^{\circ}\text{C}$, followed by solution treatment and aging. This resulted in a notable improvement in mechanical properties, with a yield strength of 868.9 MPa and an ultimate tensile strength of 878.6 MPa. Furthermore, Wang et al. [74] observed the fragmentation of primary phases in an Al-10.8Zn-2.8Mg-1.9Cu alloy during hot rolling at 380 $^{\circ}\text{C}$ and identified the extensive presence of two types of coherent GP zones (spherical GPI zones and thin platelet GPII zones), leading to superior strength.

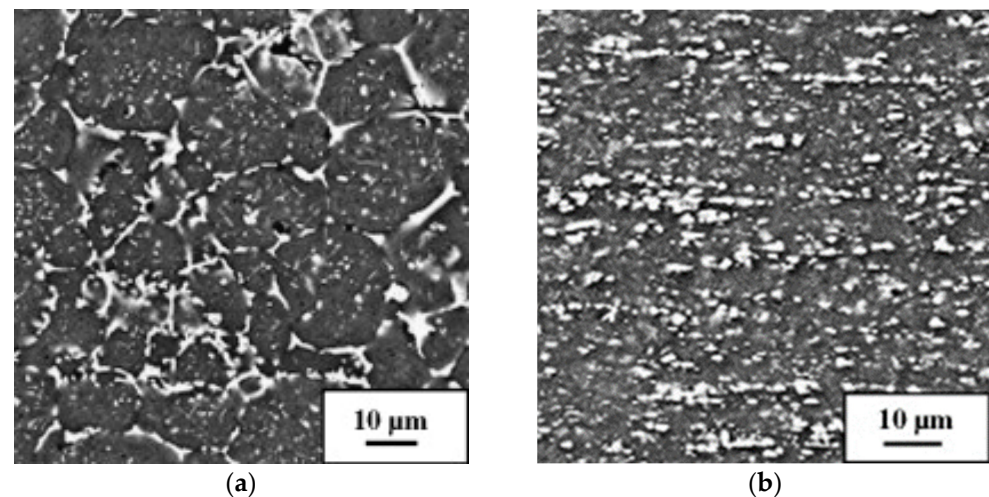


Figure 7. SEM micrographs of spray-deposited Al-10.8Zn-2.8Mg-1.9Cu alloy: (a) as deposited and (b) as hot-rolled [74].

During the hot deformation processes such as hot extrusion, forging, and hot rolling, spray-formed aluminum alloys are inevitably subjected to localized unevenness in temperature and load, leading to irregularities in microstructure and properties. For example, the friction between the spray-formed billet and the extrusion die during hot extrusion results in higher levels of deformation, deformation rates, and temperatures at the billet's surface layer compared to its central region. Similar situations are observed during the forging and rolling processes. Concurrently, grain deformation, dynamic recrystallization, and the evolution of second phases, typically associated with hot deformation parameters, frequently occur. Thus, even minor differences in these parameters may significantly affect the alloy's microstructure and properties [75–77]. Aryshenskii et al. [78] observed that the inhomogeneity of stress state, strain intensity, and strain rate in the deformation zone leads to uneven microstructure and properties in alloys processed by hot deformation. This finding has been corroborated by numerous studies. For instance, the tensile properties of forged 7010 alloy diminish gradually from the surface to the center [61]. Similarly, the interlayer structure, texture, tensile properties, and fracture toughness of rolled 7050 sheets display unevenness along the thickness direction [79]. The strength of the central layer of the hot-rolled 7055 thick plate is found to be superior to that of the surface layer [80]. Additionally, during the hot extrusion process, coarse-grained structures are prevalent in the surface layers of $2\times\times\times$, $6\times\times\times$, and $7\times\times\times$ Al alloys, with grain sizes reaching 10 to 100 times those at the center, significantly reducing the strength, toughness, and stress corrosion cracking (SCC) resistance [81–83]. To ensure product quality, it is common practice to remove areas with inferior performance or discard the entire product, leading to increased production costs [84,85]. Therefore, the inhomogeneity along the thickness direction of the plate must be fully considered when studying the effects of heat treatment and hot deformation on the microstructure and properties of spray-formed Al-Zn-Mg-Cu alloys. Appropriate methods should be implemented to mitigate the unevenness caused by hot deformation, thereby enhancing the alloy's comprehensive properties.

4. Heat Treatment of Spray-Formed Al-Zn-Mg-Cu Alloy

The heat treatment processes have a profound influence on the microstructure of the Al-Zn-Mg-Cu alloy, such as grain size, recrystallization, grain boundary morphology, precipitates, and precipitate-free zones. This significantly impacts the alloy's overall performance [86–90]. Due to the rapid solidification characteristic of spray forming, an enhanced solid solubility of alloying elements into the matrix is enabled, resulting in a notably higher solute concentration compared to traditional casting alloys. Furthermore, the diminished solute concentration gradients in the matrix, resulting from the relatively

low level of composition segregation in spray-formed Al-Zn-Mg-Cu alloys, led to reduced atomic diffusion, thus affecting the alloy's microstructure and properties. Consequently, it is imperative that an exhaustive investigation into the effects of diverse heat treatments on the microstructure, mechanical properties, and SCC resistance of the spray-formed Al-Zn-Mg-Cu alloy is performed [37,91].

4.1. Homogenization

Compared with traditional cast Al-Zn-Mg-Cu alloys, the microstructure of spray-formed Al-Zn-Mg-Cu billets exhibits exceptional homogeneity and negligible compositional segregation, leading some researchers to question if the homogenization of these billets is necessary [92,93]. However, existing studies have shown that the homogenization of spray-formed Al-Zn-Mg-Cu alloys is beneficial for promoting the precipitation of nanoscale dispersed phases such as Al_3Zr , Al_3Sc , and Al_7Cr , which is beneficial for inhibiting recrystallization and improving the comprehensive performance of the alloy. For example, Yu et al. [85] conducted an extended solution treatment (lasting for 24 h at 450 °C) on spray-formed 7055 extruded plates that had not undergone homogenization treatment. This approach resulted in superior mechanical properties, specifically, a yield strength of 608 MPa, a tensile strength of 667 MPa, and an elongation of 10%, respectively. Furthermore, Xie et al. [9] found that due to the characteristics of the spray-forming process, compared with traditional cast Al-Zn-Mg-Cu alloys, the homogenization of spray-formed alloys will result in a more uniform distribution and smaller size of the Al_3Zr dispersed phases, which better inhibits the occurrence of recrystallization. Figure 8 shows the grain structure after the hot extrusion of spray-formed and traditional cast 7055 aluminum alloys after homogenization. The extruded sample of spray-formed alloys shows a recovered, but still mainly deformed, fibrous microstructure with limited recrystallized grains as shown in Figure 8a, while the extruded sample of casted alloy shows a mainly recrystallized microstructure in Figure 8b. This difference is definitely attributed to the different contents of Al_3Zr dispersoids formed during homogenization in the two alloys. The Al_3Zr precipitates in traditional cast alloys after homogenization have uneven distribution and larger size, while those in spray-formed alloys after homogenization have homogeneous distribution and much finer size.

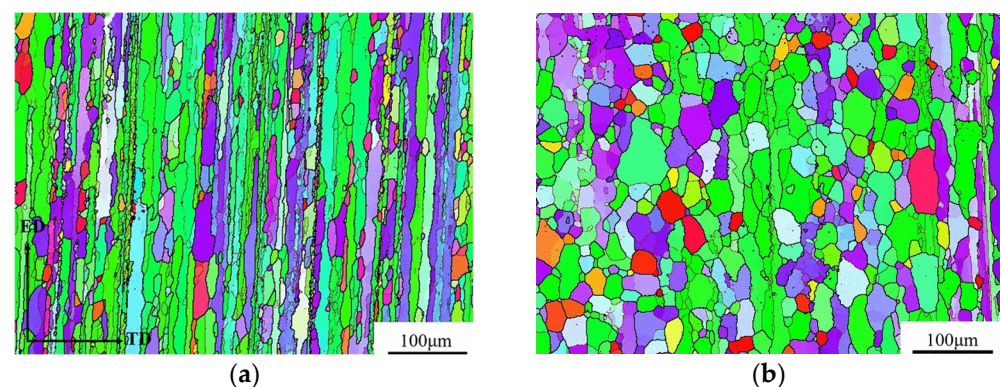


Figure 8. SEM EBSD orientation imaging maps of extruded 7055 alloy after homogenization at 470 °C/72 h: (a) spray-formed 7055 alloy and (b) conventionally cast 7055 alloy [9].

4.2. Solution Treatment

Solution treatment involves the alloy being held for a specific duration at high-temperature, to ensure the dissolution of the primary phase into the matrix, and then rapidly cooled to produce a supersaturated solid solution. The primary objective of this treatment is the elimination of the work hardening of the alloy during hot deformation and the establishment of suitable microstructure conditions for subsequent aging treatments [94]. Typically, the probability of achieving a supersaturated solid solution is enhanced by higher solution temperatures and faster quenching speeds. However, an excessively high solution

temperature leads to over burning. In that case, solution treatment is generally applied to Al-Zn-Mg-Cu alloys at approximately 470 °C. Figure 9 represents the extent of the dissolution of secondary phase particles in the solutionized alloy preserved for 3 h at 475 °C and the inserted image corresponds to the extruded condition, verifying that most of the secondary phase particles in the extruded alloy dissolved during solution treatment.

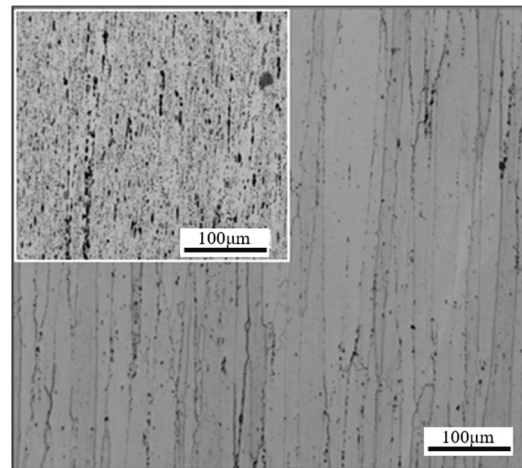


Figure 9. Optical micrograph of solutionized alloy and corresponding extruded alloy (as inserted) [37].

Notably, in spray-formed Al-Zn-Mg-Cu alloys, the high solute concentration and low concentration gradient result in a reduced unit diffusion of solute atoms, thereby decreasing diffusion efficiency. Consequently, an extended solution time becomes necessary to attain favorable solution effects [37]. The diverse re-dissolution temperatures of different second phases in Al-Zn-Mg-Cu alloys present challenges for a single solution treatment to effectively dissolve them all. As a result, the dual-stage or multi-stage solution treatment has been designed. By gradually increasing the solution temperature in steps, the final solution treatment can be carried out at higher temperature while avoiding over burning, thereby ultimately improving the solution effect.

4.3. Aging

The predominant strengthening mechanism for Al-Zn-Mg-Cu alloys, precipitation hardening [65,95,96], is achieved through the solution treatment to form a supersaturated solid solution followed by the aging process to precipitate abundant strengthened phases [97–100]. Common aging treatments include single-stage aging (T6), double-stage aging (T7) [101], and retrogression and re-aging (RRA) [102]. The aging temperature and time are the crucial parameters that impact precipitation behaviors. During aging at temperatures ranging from 20 to 100 °C, Guinier–Preston (GP) zones are initially precipitated in Al-Zn-Mg-Cu alloys [103], transforming into the η' phase with prolonged aging time. Aging at temperatures between 120 and 170 °C primarily results in the precipitation of the η' phase [104], which gradually transforms into the η phase over extended aging periods, while direct precipitation of the η phase [105], coarsening with increasing aging time, is led by aging above 170 °C [106,107]. Typically, the highest strength for Al-Zn-Mg-Cu alloys is achieved through aging at 120 °C for 24 h, known as peak aging [108].

For spray-formed Al-Zn-Mg-Cu alloys, a shorter time is required to reach peak aging compared to traditional casting ones, which is associated with their solute element content. Current research has indicated that the time required for the alloy to reach peak aging is mainly influenced by the content of the alloying element Zn [109], and is related to the driving force for precipitation. The driving force for precipitation, denoted as Δg , can be calculated using the following formula [110]:

$$\Delta g = -\frac{KT}{V_{at}} \ln\left(\frac{c}{c_{eq}}\right) \quad (1)$$

In Formula (1), K represents the Boltzmann constant; T stands for the thermodynamic temperature; V_{at} denotes the volume of solute atoms (considered constant); c represents the molar concentration of solute in the matrix; and c_{eq} signifies the molar concentration of solute at equilibrium. The driving force for precipitation is determined by the solute concentration in the alloy matrix when the aging temperature is fixed. In spray-formed alloys, a greater influx of solute atoms into the matrix during solution treatment results from the higher content of alloying elements, leading to a higher concentration within the matrix, which amplifies the driving force for precipitation, thereby accelerating the time to reach peak aging. It was observed by Tian et al. [64] that a tensile strength of 796 MPa was achieved by the extruded plate of spray-formed 7034 after undergoing dual solution treatment and aging. A study was conducted by Li et al. [35] on a spray-formed Al-8.15Zn-2.46Cu-1.97Mg-0.15Fe-0.13Zr-0.04Cr alloy, which was subjected to single-stage aging (T6), two-stage aging (T7), and non-isothermal retrogression and re-aging (NRRRA) processes. The variations in the composition of precipitation phases resulting from different aging treatments are depicted in Figure 10. The findings revealed that outstanding comprehensive mechanical properties were demonstrated by the alloy after NRRRA treatment, with its tensile strength approaching that of the T6 state, an elongation of 10.5%, and much better corrosion resistance than that of the T6 state alloy.

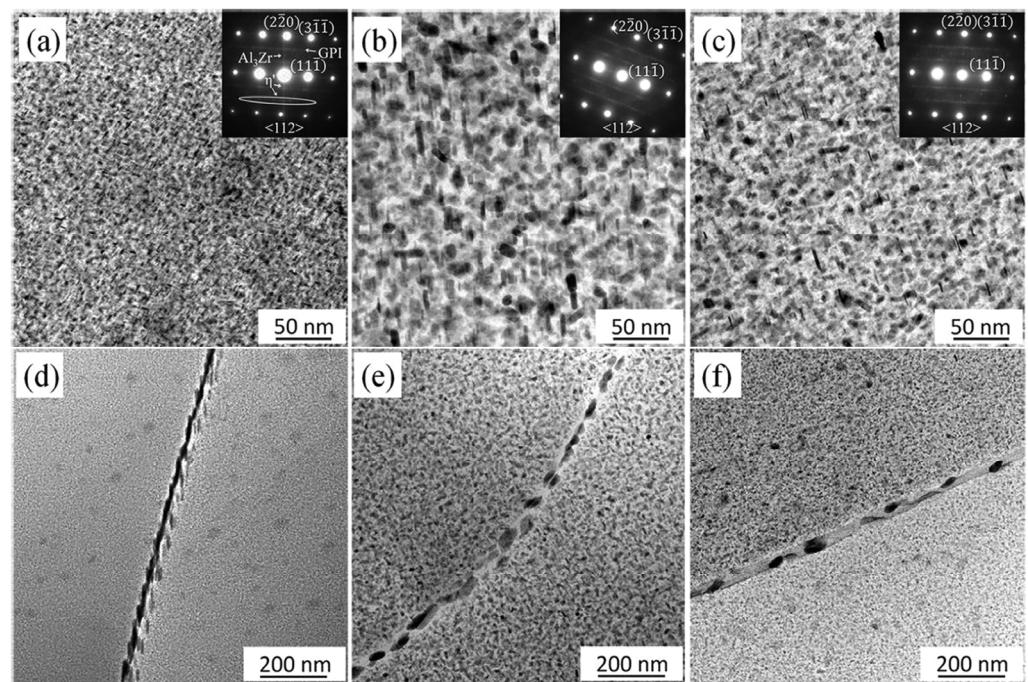


Figure 10. TEM images of the specimens under different aging conditions: (a,d) peak-aging; (b,e) over-aging; (c,f) NRRRA [24].

5. Second Phases and Their Influence on the Recrystallization Behavior of Spray-Formed Al-Zn-Mg-Cu Alloys

5.1. Second Phases

In spray-formed Al-Zn-Mg-Cu alloys, three main types of second phases are present: the primary phase, dispersoids, and precipitates during aging (including intragranular and intergranular second phases), distinguished by their formation time and size [111,112]. The second phases in spray-formed Al-Zn-Mg-Cu alloys may differ from those in traditional casting ones, due to the rapid solidification, high alloying, and uniform composition without segregation characteristics attributed to the spray-forming process.

5.1.1. Primary Phases

The primary phase is formed during the solidification of the alloy melt and is located at grain boundaries or within grains. They are primarily composed of the main alloying element Al and impurity elements such as Fe and Si, mainly including the S phase (Al_2CuMg), Fe-containing phase ($\text{Al}_7\text{Cu}_2\text{Fe}$), Si-containing phase, and primary coarse Al_3Zr , with sizes typically varying from 0.1 to 30 μm . The primary phase, being a detrimental brittle phase for the alloy, includes certain phases capable of re-dissolving into the matrix during subsequent heat treatment [87]. The spray-forming process is conducted under a protective environment of high-pressure inert gas, which can mitigate the introduction of impurities such as Fe and Si, thereby reducing the presence of impurity phases like the Fe-bearing phase ($\text{Al}_7\text{Cu}_2\text{Fe}$) and Si-containing phase. Moreover, the solubility of alloying elements is enhanced by the rapid solidification in the spray-forming process, consequently minimizing the precipitation of coarse primary phases [92,113]. It is noteworthy that the absence of the S phase (Al_2CuMg) in spray-formed Al-Zn-Mg-Cu alloys is reported in some studies, while the presence of the S phase in the spray-formed 7055 alloy has been detected by Si and Yang et al. [114,115].

5.1.2. Precipitates during Aging

Throughout the aging process, nanophases are precipitated within grains and at grain boundaries in Al-Zn-Mg-Cu alloys. Notably, the nano-scale strengthening phase within grains, exhibiting coherence or semi-coherence with the matrix, serves as the primary reinforcement phase, while the corrosion resistance is influenced by grain boundary precipitation (GBP) [116]. The typically established aging precipitation sequence for Al-Zn-Mg-Cu alloys is as follows: supersaturated solid solution (SSS) \rightarrow GP zone \rightarrow η' phase (MgZn_2) \rightarrow stable η phase (MgZn_2) [106,117–119]. The three types of precipitates in spray-formed Al-Zn-Mg-Cu alloys are presented in Table 2. The disc-shape η' precipitates, with diameters typically spanning 10 to 20 nm and thicknesses generally below 5 nm, have four variants which are shown in Figure 11. The shape of η' appearing in TEM images could adopt needle-like or plate-like shapes depending on the observed plane. Equilibrium phase η phases are often manifested as disc-shaped structures, with diameters exceeding 50 nm and thicknesses surpassing 10 nm [120]. Furthermore, the precipitation of T' phase ($\text{Mg}_{32}(\text{Al}, \text{Zn})_{49}$) and T phase ($\text{Mg}_{32}(\text{Al}, \text{Zn})_{49}$) may be led by elevated Mg content in the alloy ($\text{Zn}/\text{Mg} < 2.2$ wt.%) [121,122]. The morphologies of the η' and η phases are depicted by transmission electron microscope (TEM) images in Figure 12, highlighting discernible disparities in their shapes and sizes.

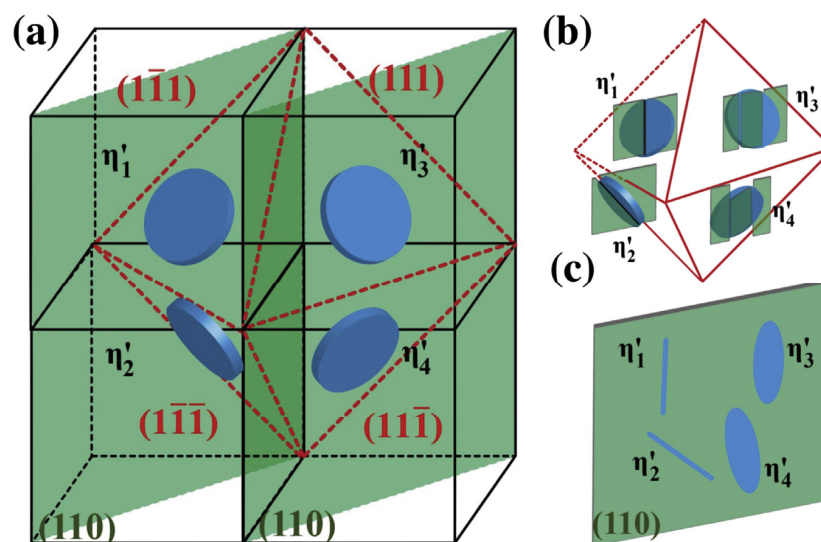


Figure 11. (a) Four variants of η' precipitates marked blue (i.e., η'_1 to η'_4) grow on $[111,123]_{\text{Al}}$ habit planes, and the observed plane via TEM is the $(110)_{\text{Al}}$ plane in green. (b) The intersections between

four variants of η' precipitates and the $(110)_{\text{Al}}$ plane of the Al matrix are sketched. (c) Along the observation of the $(110)_{\text{Al}}$ zone axis, two variants of η' precipitates (i.e., η'_1 and η'_2) are shown as edge-on configurations, and the others (i.e., η'_3 and η'_4), as ellipse-like morphologies [107].

Table 2. The three types of precipitated phases of spray-formed Al-Zn-Mg-Cu alloys.

Name	Sort	Coherent	Lattice Constant (nm)	Pattern
GP zone	GP(I) zone, GP(II) zone	Coherence		Globosity
η' phase		Coherence, semi-coherence	Hexagonal $a_{\eta'} = 0.496$ $c_{\eta'} = 1.403$	Circular
η phase		Incoherence	Hexagonal $a_{\eta} \approx 0.5221$ $c_{\eta} \approx 0.8567$	Stick circular

The mechanical properties of Al-Zn-Mg-Cu alloys are significantly influenced by the content of Zn and Mg elements [124]. Theoretically, the strength of these alloys can be augmented by approaching theoretical limits of Zn content and maintaining an appropriate Cu to Mg ratio; however, practical constraints arising from alloy solubility limit this pursuit. Specifically, the development of coarse reticular second phases, leading to diminished mechanical performance, is often culminated by Zn content exceeding 8 wt.% in conventional cast alloys [125,126]. Contrastingly, the solubility of alloying elements is enhanced by the spray-forming process, thereby facilitating the precipitation of strengthening η' phases during subsequent heat treatment and aging processes, ultimately elevating the mechanical properties [127,128].

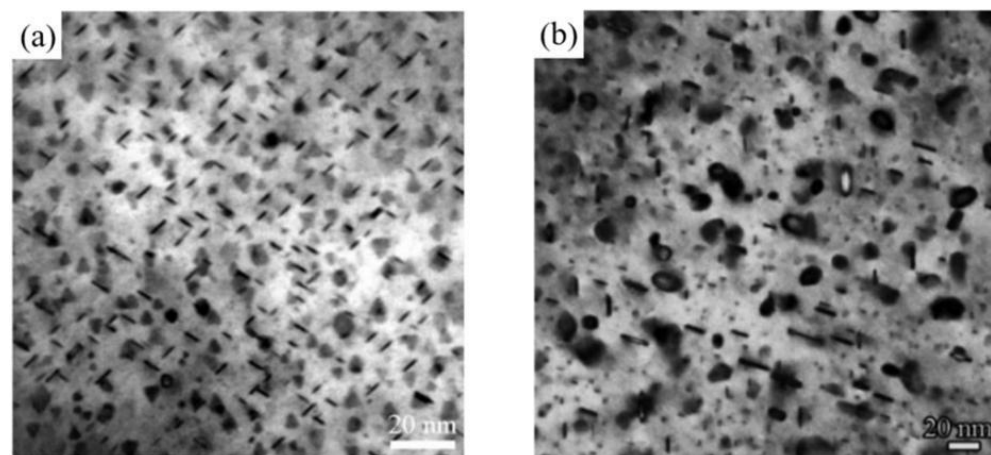


Figure 12. TEM images of (a) η' and (b) η [128].

5.1.3. Dispersoids

During high-temperature heat treatments such as homogenization and solution treatment, dispersoids are formed within the grains, especially in alloys containing Sc, Zr, or rare earth elements. These dispersoids, which include fine Al_3Zr , Al_3Sc or Al_3Re , typically range in size from 0.03 to 0.5 μm . Once precipitated, these dispersoids, possessing stable structures, become challenging to re-dissolve into the matrix [129]. The presence of these dispersoids effectively hinders dislocation movement and inhibits grain boundary migration during hot deformation and solution treatment, thereby suppressing recrystallization and grain growth. This refinement results in grain size reduction and a consequent enhancement of the mechanical properties [88]. Due to the high cost of Sc, research has predominantly focused on the influence of Zr on the properties of Al-Zn-Mg-Cu aluminum alloys [130–133]. It is generally accepted that the addition of 0.05–0.15 wt.% Zr can result

in the formation of the fine intermetallic compound Al_3Zr [134]. It was noted by Xie et al. [9] that the distribution of Zr within the grain is uneven in the as-cast 7055 alloy, while it is uniformly distributed in the spray-formed 7055 alloy billet. This disparity results in differences in the precipitation behavior of Al_3Zr after two-stage homogenization at $350^\circ\text{C}/5\text{ h} + 470^\circ\text{C}/24\text{ h}$ (at a heating rate of $30^\circ\text{C}/\text{h}$). In the spray-formed 7055 alloy, a large number of uniformly distributed, nanoscale Al_3Zr particles are precipitated throughout the entire grain, whereas in the as-cast 7055 alloy, Al_3Zr particles tend to aggregate at the center of the grain.

5.2. The Influence of the Second Phases on the Recrystallization Behavior of Spray-Formed Al-Zn-Mg-Cu Alloy

The composition, size, shape, and quantities of second phase particles in Al-Zn-Mg-Cu alloys are known to have varying impacts on the nucleation and growth of recrystallization, as shown in Figure 13, consequently influencing its properties [135,136]. The existence of fine second phase particles is conspicuously noted to induce a Zener pinning effect, effectively impeding the movement of grain boundaries and dislocations, thereby suppressing the nucleation and growth of recrystallized grains [137].

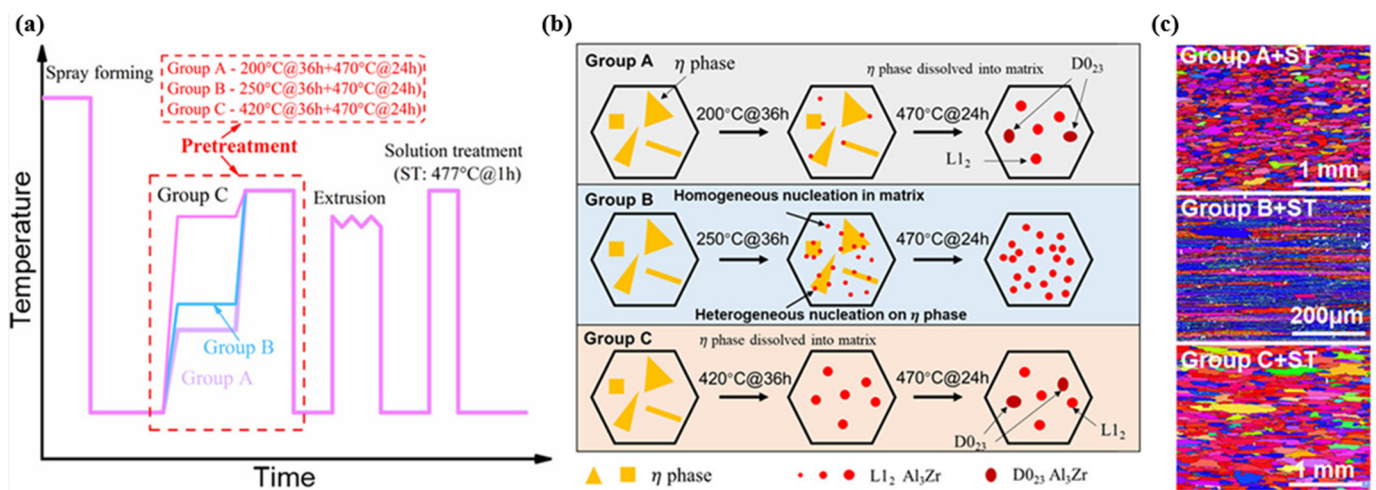


Figure 13. (a) Schematic diagram of different treatments; (b) schematic showing the evolution of η phases and heterogeneous nucleation mechanism of Al_3Zr precipitates during pretreatments; and (c) EBSD IPF maps of as-quenched spray-formed 7050 alloys after different treatments shown in (a) [136].

The Zener pinning force (P_z) is expressed using the following formula [138]:

$$P_z = \frac{3f_v\gamma_{AB}}{2r} \quad (2)$$

In Formula (2), f_v is defined as the percentage of the total volume occupied by the second phase particles, γ_{AB} represents the interfacial tension, and r is identified as the radius of the second phase particles. When the coarse second phase particles exceed the critical nucleation size, a significant misorientation between the second phase particles and the surrounding matrix is noted, resulting in a high dislocation density within the region of strong lattice distortion. This high dislocation density is observed to provide a substantial driving force for grain boundary migration, promoting recrystallization nucleation and accelerating the recrystallization behavior.

The critical nucleation size (d) of the second phase is calculated using the following formula [139]:

$$d \geq \frac{2\gamma}{3(P_D - P_z)} \quad (3)$$

In Formula (3), γ represents the grain boundary energy, P_D corresponds to the recrystallization driving force associated with deformation stored energy, and P_Z is the Zener pinning force required to separate the grain boundaries from the second phase. According to Nes et al. [140], the shape and spatial distribution of second phase particles, apart from their size, were discovered to have a considerable impact on the Zener pinning force, thereby strongly affecting recrystallization and grain growth. Furthermore, an extensive EBSD analysis conducted by She et al. [141] on the influence of different types of coarse second phases with varying Fe and Si content on recrystallization in hot deformed 7055 revealed that irregular Mg_2Si and Al_7Cu_2Fe particles with aspect ratios of 3–4 induced a severe degree of local non-uniform deformation, leading to a stronger promotion effect on recrystallization. In contrast, rod-like Al_7Cu_2Fe particles with aspect ratios greater than six were found to cause the most significant local non-uniform deformation. However, due to their shape, local non-uniform deformation was confined within their deformation area, resulting in less promotion effect on recrystallization compared to irregular Mg_2Si and Al_7Cu_2Fe particles with aspect ratios of 3–4. This suggests that the extent of local non-uniform deformation induced by these second phases aligns with their promotion effect on recrystallization. Thus, to refine grain size and enhance the performance of aluminum alloys, the blunting, spheroidizing of needle-like, skeletal, and plate-like second phase particles and their uniform dispersion are generally necessary.

5.3. The Influence of the Grain Size on the Mechanical Properties

The small secondary phase in the alloy hinders recrystallization, resulting in smaller grain size and better grain boundary strengthening effect, leading to an increase in the strength of the alloy. This is because the grain boundaries between differently oriented grains can strongly hinder the motion of dislocations towards neighboring grains, causing dislocations to accumulate at the grain boundaries and generating an interaction force with the grain boundaries, resulting in the formation of the stress field near the grain boundaries. At the same time, this stress field can further hinder the motion of dislocations, resulting in a strengthening effect and improving the strength of the alloy [123]. This strengthening effect is known as grain boundary strengthening, also known as fine grain strengthening. The grain-boundary strengthening mechanism is usually described by the Hall–Petch equation [142,143]:

$$\sigma_{\sigma b} = \sigma_{\alpha} + kd^{-1/2} \quad (4)$$

where $\sigma_{\sigma b}$ is the contribution of grain boundary strengthening to the strength of the alloy, d is the average grain diameter, σ_{α} is the strength of the Al matrix and k is the Hall–Petch slope. From the formula, it can be seen that the smaller the grain size of the alloy, the more beneficial to the improvement of its strength. The spray-forming technique can effectively refine the grain size of aluminum alloys, thereby greatly enhancing their mechanical properties.

In summary, large-sized second phases found in spray-formed 7055, such as the S phase (Al_2CuMg), η phase ($MgZn_2$), T phase ($Mg_{32}(Al, Zn)_{49}$), Fe-containing phase (Al_7Cu_2Fe), and Si-containing phase, are observed to promote recrystallization and should be minimized. Conversely, for the relatively smaller second phases that precipitate during aging, such as the GP zone and η' phase, as well as the Al_3Zr that precipitate during heat treatment [144,145], it is advisable to judiciously control the heat treatment parameters to achieve a dispersed distribution. This strategy is aimed at hindering recrystallization and refining grain size, thereby enhancing the mechanical properties.

6. High-Temperature Performance of Spray-Formed Al-Zn-Mg-Cu Alloy

Despite the superior room temperature mechanical properties of spray-formed Al alloy compared to the traditional casting one, more stringent high-temperature performances have been required by the rapid development in the aerospace industry. Aluminum alloys are prone to recovery and recrystallization owing to the relatively low melting point and high stacking fault energy. Rapid coarsening or dissolution of phases above

200 °C is experienced by many precipitation-hardened Al alloys, making their utilization at temperatures exceeding 200 °C challenging. Taking the 7075 alloy as an example, its high-temperature tensile strength at 200 °C and 300 °C is only approximately 30% and 10% of its room temperature strength, respectively [146]. The improvement of the high-temperature performance of Al-Zn-Mg-Cu series aluminum alloys, especially in aerospace applications, has become a focal point of research. The high-temperature performance of the 7075-T6 alloy under different strain rates from room temperature to 450 °C was studied by Rong et al. [147], who sought to propose an improved continuous fracture model to describe and predict the fracture behavior of the 7075 alloy at high temperatures. It was found by Guo et al. [148] that concurrent work hardening, dynamic recovery, and dynamic recrystallization at 200 °C were exhibited by the hot-rolled Al-Zn-Mg-Cu alloy; below 200 °C, work hardening emerged as the primary deformation mechanism, while above 200 °C, dynamic recovery and dynamic recrystallization became the main deformation mechanisms, and the microstructure became sensitive to the flow strain rate. A decrease in the flow stress of 7150 during isothermal hot compression within the temperature range of 325–425 °C and a strain rate range of 0.01^{-1} s^{-1} was observed by Jiang et al. [149]. This decrease was correlated with elevated temperatures, increased cumulative strain, as well as reduced strain rates and deformation. The high-temperature performance (room temperature to 175 °C) of the forged 7085-T74 alloy was investigated by Dai et al. [150], who discovered a transition in the fracture mode of the alloy from mixed transgranular and intergranular fracture to a pure transgranular fracture as the temperature increased to 150 °C.

Currently, the enhancement of heat resistance is primarily achieved by forming a high-volume fraction of thermally stable strengthening phases within the matrix, utilizing the pinning effect of these phases on dislocations and grain boundaries to enhance the high-temperature performance. The addition of rare earth elements or transition metal elements (such as Sc, Er, and Zr), along with suitable aging treatments, leads to the formation of dispersed phases (Al_3Sc , Al_3Zr , etc.) with outstanding thermal stability and anti-coarsening capabilities, thus improving the alloy's high-temperature performance [151]. It was found by Lang et al. [152] that secondary $\text{Al}_3(\text{Sc}, \text{Zr})$ particles formed in Al-Zn-Mg-Cu alloys with added trace amounts of Sc hindered dislocation movement during high-temperature deformation, effectively enhancing the high-temperature performance. Zhai et al. [153] discovered that the formation of high-melting point $\text{Al}_{10}\text{Cu}_7\text{Sm}_2$ phases in Al-Zn-Mg-Cu-Zr alloys with Sm addition anchored grain boundaries during high-temperature deformation, thereby improving the high-temperature performance. Furthermore, the high-temperature performance of Al-Zn-Mg-Cu alloys, similar in composition to the 7055 alloy but without Zr, was studied by Han et al. [154]. Their results indicated that increasing the oxygen content during the alloy preparation process allowed the formation of $\gamma\text{-Al}_2\text{O}_3$, which hindered dislocation movement and grain boundary migration, thus enhancing the high-temperature performance.

In addition, the low solid solubility caused by traditional casting processes is compensated by rapid solidification technology [155–157], which enhances the supersaturated solid solubility of alloying elements in the aluminum matrix and promotes the formation of thermally stable fine dispersed phases [158]. The preparation techniques commonly used for the rapid solidification of heat-resistant aluminum alloys mainly include planar flow casting [159], gas atomization [160], and spray forming [161]. Research on the high-temperature (room temperature to 400 °C) tensile properties of spray-formed 7055-T6 and 7055-T74 alloys by Khan et al. [57] indicates that a maximum environmental temperature of 200 °C can be withstood by the structural components of the 7055-T6 alloy. Wang et al. [162] found that in the spray-formed Al-8.5Fe-1.1V-1.9Si heat-resistant alloy, the formation of coarse and brittle primary silicon crystals and eutectic phases between dendrites was inhibited due to the low solidification rate, while dispersed fine spherical $\text{Al}_{12}(\text{Fe}, \text{V})_3\text{Si}$ particles with exceptional thermal stability were distributed in the matrix. Such microstructure endows the alloy with excellent room temperature and high-temperature mechanical

properties. Therefore, one of the important approaches for developing high-strength and high-temperature resistant Al-Zn-Mg-Cu alloys is the spray-forming technique combined with microalloying.

7. Summary and Prospect

1. Several advantages are offered by the Al-Zn-Mg-Cu alloys produced by spray forming rather than traditional casting, including uniform composition, fine grain size, low internal stress, and high alloying capacity. Nevertheless, the performance of spray-formed alloys can be negatively impacted by the presence of significant porosity. This issue can be resolved through hot deformation processes such as hot extrusion and forging, which refine the microstructure and reduce the porosity. Different heat treatments like homogenization, solution treatment, and aging, can be optimized, further enhancing the material's properties.
2. Despite the validation of spray-formed Al-Zn-Mg-Cu alloys in some application scenarios, the technique is still limited by a lack of material diversity and narrow application scope. To address current challenges, both the material design and new applications of spray-formed aluminum ought to be explored, for example, high alloyed Al-Zn-Mg-Cu alloys, aluminum alloys for high temperature applications, high toughness aluminum alloys, etc.
3. In order to develop spray-formed aluminum alloys with superior performance suitable for practical use, it becomes imperative to conduct comprehensive numerical simulations and optimizations of the manufacture process. This ensures that deformation processing and heat treatment are optimized, resulting in enhanced outcomes. Real-time monitoring and intelligent control of the spray-forming process should also be exploited to improve the quality of spray-formed products.

Author Contributions: Conceptualization, L.C. and X.W.; writing—original draft preparation, X.L., Z.Z. and M.B.; writing—review and editing, Z.Z. and M.B.; supervision, L.C. and X.W.; visualization, X.L.; project administration, X.W.; funding acquisition, L.C. All authors have read and agreed to the published version of the manuscript.

Funding: This research was funded by Natural Science Foundation of Chongqing, China (CSTB2022NSCQLZX0002), Chongqing Key Project for Technological Innovation and Application (CSTB2022TIAD-KPX0073), and the Opening Project of State Key Laboratory for Advanced Metals and Materials (2022-Z03 and 2020-ZD02).

Data Availability Statement: Not applicable.

Conflicts of Interest: The authors declare that they have no known competing financial interests or personal relationships that could have appeared to influence the work reported in this paper.

References

1. Feng, D.; Zhang, X.M.; Liu, S.D.; Wang, T.; Wu, Z.Z.; Guo, Y.W. The Effect of Pre-Ageing Temperature and Retrogression Heating Rate on the Microstructure and Properties of AA7055. *Mater. Sci. Eng. A* **2013**, *588*, 34–42. [[CrossRef](#)]
2. Teng, G.B.; Liu, C.Y.; Ma, Z.Y.; Zhou, W.B.; Wei, L.L.; Chen, Y.; Li, J.; Mo, Y.F. Effects of Minor Sc Addition on the Microstructure and Mechanical Properties of 7055 Al Alloy During Aging. *Mater. Sci. Eng. A* **2018**, *713*, 61–66. [[CrossRef](#)]
3. Zhang, C.S.; Zhao, G.Z.; Ming, F.L.; En, C.B.; Liang, C.; Guo, Q.Z. Effects of Single- and Multi-Stage Solid Solution Treatments on Microstructure and Properties of as-Extruded AA7055 Helical Profile. *Trans. Nonferrous Met. Soc. China* **2021**, *31*, 1885–1901. [[CrossRef](#)]
4. Wang, H.; Zhang, H.M.; Cui, Z.S.; Chen, Z.; Chen, D. Compressive Response and Microstructural Evolution of in-Situ TiB_2 Particle-Reinforced 7075 Aluminum Matrix Composite. *Trans. Nonferrous Met. Soc. China* **2021**, *31*, 1235–1248. [[CrossRef](#)]
5. He, K.Z.; Li, Q.; Liu, S.D.; Zhang, X.M.; Zhou, K.C. Influence of Pre-Stretching on Quench Sensitive Effect of High-Strength Al–Zn–Mg–Cu–Zr Alloy Sheet. *J. Cent. South Univ.* **2021**, *28*, 2660–2669. [[CrossRef](#)]
6. Zhao, Y.; Wang, Q.Z.; Chen, H.B.; Yan, K. Microstructure and Mechanical Properties of Spray Formed 7055 Aluminum Alloy by Underwater Friction Stir Welding. *Mater. Des.* **2014**, *56*, 725–730. [[CrossRef](#)]
7. Salvo, G.J.; Afonso, R.M. Fatigue Strength and Microstructure Evaluation of Al 7050 Alloy Wires Recycled by Spray Forming, Extrusion and Rotary Swaging. *Trans. Nonferrous Met. Soc. China* **2020**, *30*, 3195–3209. [[CrossRef](#)]

8. Liu, S.D.; Zhang, Y.; Liu, W.J.; Deng, Y.L.; Zhang, X.M. Effect of Step-Quenching on Microstructure of Aluminum Alloy 7055. *Trans. Nonferrous Met. Soc. China* **2010**, *20*, 1–6. [[CrossRef](#)]
9. Xie, Z.Q.; Jia, Z.H.; Xiang, K.Y.; Kong, Y.P.; Li, Z.G.; Fan, X.; Ma, W.T.; Zhang, H.; Lin, L.; Marthinsen, K.; et al. Microstructure Evolution and Recrystallization Resistance of a 7055 Alloy Fabricated by Spray Forming Technology and by Conventional Ingot Metallurgy. *Metall. Mater. Trans. A Phys. Metall. Mater. Sci.* **2020**, *51*, 5378–5388. [[CrossRef](#)]
10. Mondal, C.; Mukhopadhyay, A.K.; Raghu, T.; Varma, V.K. Tensile Properties of Peak Aged 7055 Aluminum Alloy Extrusions. *Mater. Sci. Eng. A* **2007**, *454–455*, 673–678. [[CrossRef](#)]
11. Henein, H.; Uhlenwinkel, V.; Fritsching, U. *Metal Sprays and Spray Deposition*; Springer International Publishing: Cham, Switzerland, 2017; pp. 379–406.
12. Lavernia, E.J.; Grant, N.J. Spray Deposition of Metals: A Review. *Mater. Sci. Eng.* **1988**, *98*, 381–394. [[CrossRef](#)]
13. Evans, J.W.; Jonghe, L.C. *The Production and Processing of Inorganic Materials*; Springer International Publishing: Cham, Switzerland, 2016; pp. 477–511.
14. Zhang, G.W.; Zhen, Z.C.; Wei, C.; Hai, Y.X.; Jing, Z.; Guo, A.Z.; Li, M.; Gang, C. The Microstructure and Mechanical Properties of Super-High Strength Al Alloys by Spray Forming. *Adv. Mater. Res.* **2012**, *535–537*, 909–914. [[CrossRef](#)]
15. Reddy, B.V.R.; Maity, S.R.; Pandey, K.M. Characterization of Spray Formed Al-Alloys—A Review. *Rev. Adv. Mater. Sci.* **2019**, *58*, 147–158. [[CrossRef](#)]
16. Wang, F.; Yang, B.; Duan, X.J.; Xiong, B.Q.; Zhang, J.S. The Microstructure and Mechanical Properties of Spray-Deposited Hypereutectic Al-Si-Fe Alloy. *J. Mater. Process. Technol.* **2003**, *137*, 191–194. [[CrossRef](#)]
17. Ha, T.K.; Park, W.J.; Ahn, S.; Chang, Y.W. Fabrication of Spray-Formed Hypereutectic Al-25Si Alloy and Its Deformation Behavior. *J. Mater. Process. Technol.* **2002**, *130–131*, 691–695. [[CrossRef](#)]
18. Kim, W.J.; Yeon, J.H.; Lee, J.C. Superplastic Deformation Behavior of Spray-Deposited Hyper-Eutectic Al-25Si Alloy. *J. Alloys Compd.* **2000**, *308*, 237–243. [[CrossRef](#)]
19. Wu, Y.; Cassada, W.A.; Lavernia, E.J. Microstructure and Mechanical Properties of Spray-Deposited Al-17Si-4.5Cu-0.6Mg Wrought Alloy. *Metall. Mater. Trans. A-Phys. Metall. Mater. Sci.* **1995**, *26*, 1235–1247. [[CrossRef](#)]
20. Estrada, J.L.; Duszczyn, K.J. Characteristics of Rapidly Solidified Al-Si-X Preforms Produced by the Osprey Process. *J. Mater. Sci.* **1990**, *25*, 1381–1391. [[CrossRef](#)]
21. Su, Y.H.; Frank, C.S.; Chiang, S.; Tsao, C.Y.A. Extrusion Characteristics of Spray-Formed Ac9a Aluminum Alloy. *Mater. Sci. Eng. A* **2004**, *364*, 305–312. [[CrossRef](#)]
22. Chiang, C.H.; Tsao, C.Y.A. Workability of Spray-Formed Al/Sip Metal Matrix Composites. *Key Eng. Mater.* **2003**, *249*, 189–194. [[CrossRef](#)]
23. Saha, D.; Sumanth, S.; Diran, A.; Makhlof, M.M. Casting of Aluminum-Based Wrought Alloys Using Controlled Diffusion Solidification. *Metall. Mater. Trans. A-Phys. Metall. Mater. Sci.* **2004**, *35*, 2174–2180. [[CrossRef](#)]
24. Lee, J.S.; Jung, J.Y.; Lee, E.S.; Park, W.J.; Ahn, S.; Kim, N.J. Microstructure and Properties of Titanium Boride Dispersed Cu Alloys Fabricated by Spray Forming. *Mater. Sci. Eng. A* **2000**, *277*, 274–283. [[CrossRef](#)]
25. Ferrarini, C.E.; Bolfarini, C.; Kiminami, C.S.; Botta, W.J. Microstructure and Mechanical Properties of Spray Deposited Hypoeutectic Al-Si Alloy. *Mater. Sci. Eng. A* **2004**, *375*, 577–580. [[CrossRef](#)]
26. Desantis, M. Structure and Properties of Rapidly Solidified Ultrahigh Strength Al-Zn-Mg-Cu Alloys Produced by Spray Deposition. *Mater. Sci. Eng. A* **1991**, *141*, 103–121. [[CrossRef](#)]
27. Sharma, M.M. Microstructural and Mechanical Characterization of Various Modified 7xxx Series Spray Formed Alloys. *Mater. Charact.* **2008**, *59*, 91–99. [[CrossRef](#)]
28. Jia, Y.; Cao, F.; Ning, Z.; Guo, S.; Ma, P.; Sun, J. Influence of Second Phases on Mechanical Properties of Spray-Deposited Al-Zn-Mg-Cu Alloy. *Mater. Des.* **2012**, *40*, 536–540. [[CrossRef](#)]
29. Gingell, A.D.B.; King, J.E. Comparison of Crack Growth Behaviour between Spray-Formed and Commercial Plate Al-Zn-Mg-Cu Alloy 7150. *Mater. Sci. Forum* **1996**, *217–222*, 1605–1610. [[CrossRef](#)]
30. Guo, S. Solidification Behavior and Microstructure Evolution of Spray Deposited Al-Zn-Mg-Cu Alloy during Hot Working Process. Ph.D. Thesis, Harbin Institute of Technology, Harbin, China, 2011. (In Chinese)
31. Zhang, Y.A.; Xiong, B.Q.; Wei, Q.; Shi, L.K.; Ma, M.T. Preparation of High Performance Aluminum Alloy Materials by Spray Forming. *Mater. Mech. Eng.* **2001**, *25*, 22–25. (In Chinese)
32. Shen, J.; Song, G.S.; Zeng, S.Y.; Jiang, Z.L.; Li, Q.C. The microstructure and properties of high-strength aluminum alloy materials deposited by atomization. *Chin. J. Nonferrous Met.* **1994**, *4*, 82–84. (In Chinese)
33. Pan, Y.X. Performance of spray formed 7055 aluminum alloy for helicopter hub materials. *J. Netshape Form. Eng.* **2017**, *9*, 193–197. (In Chinese)
34. Bai, B.C.; Wan, C.P.; Zhang, X.Y.; Chen, W. Study on the microstructure and properties of Al Zn Mg Cu alloy large billets prepared by spray deposition. *J. Aeronaut. Mater.* **2007**, *27*, 11–14. (In Chinese)
35. Li, L.; Wei, L.J.; Xu, Y.J.; Mao, L.; Wu, S.J. Study on the Optimizing Mechanisms of Superior Comprehensive Properties of a Hot Spray Formed Al-Zn-Mg-Cu Alloy. *Mater. Sci. Eng. A* **2019**, *742*, 102–108. [[CrossRef](#)]
36. Xiang, K.Y.; Lei, X.C.; Ding, L.P.; Jia, Z.H.; Yang, X.F.; Liu, Q. Optimizing Mechanical Property of Spray Formed Al-Zn-Mg-Cu Alloy by Combination of Homogenization and Warm-Rolling. *Mater. Sci. Eng. A* **2022**, *846*, 143248. [[CrossRef](#)]

37. Ditta, A.; Wei, L.J.; Xu, Y.J.; Wu, S.J. Effect of Hot Extrusion and Optimal Solution Treatment on Microstructure and Properties of Spray-Formed Al-11.3Zn-2.65Mg-1Cu Alloy. *J. Alloys Compd.* **2019**, *797*, 558–565. [[CrossRef](#)]
38. Ditta, A.; Wei, L.J.; Li, L.; Xu, Y.J.; Naseem, K.; Wu, S.J. Microstructure and Mechanical Properties of Spray-Formed High Zn-Containing Al-Zn-Mg-Cu Alloy. In Proceedings of the 2019 16th International Bhurban Conference on Applied Sciences and Technology (IBCAST), Islamabad, Pakistan, 8–12 January 2019.
39. Li, H.H.; Cao, F.Y.; Guo, S.; Ning, Z.L.; Liu, Z.Y.; Jia, Y.D.; Scudino, S.; Gemming, T.; Sun, J.F. Microstructures and Properties Evolution of Spray-Deposited Al-Zn-Mg-Cu-Zr Alloys with Scandium Addition. *J. Alloys Compd.* **2017**, *691*, 482–488. [[CrossRef](#)]
40. Wang, Z.P.; Wang, M.L.; Li, Y.G.; Xiao, H.Y.; Chen, H.; Geng, J.W.; Li, X.F.; Chen, D.; Wang, H.W. Effect of Pretreatment on Microstructural Stability and Mechanical Property in a Spray Formed Al-Zn-Mg-Cu Alloy. *Mater. Des.* **2021**, *203*, 109618. [[CrossRef](#)]
41. Wei, L.J.; Han, B.S.; Ye, F.; Ditta, A.; Li, L.; Xu, Y.Y.; Wu, S.J. Influencing Mechanisms of Heat Treatments on Microstructure and Comprehensive Properties of Al-Zn-Mg-Cu Alloy Formed by Spray Forming. *J. Mater. Res. Technol.-JMRT* **2020**, *9*, 6850–6858. [[CrossRef](#)]
42. Su, R.M.; Qu, Y.; Li, R.; Li, R. Study of Ageing Treatment on Spray Forming Al-Zn-Mg-Cu Alloy. *Appl. Mech. Mater.* **2012**, *217*, 1835–1838. [[CrossRef](#)]
43. Xiong, B.Q.; Zhang, Y.G.; Zhu, B.H.; Liu, H.W.; Zhang, Z.H.; Shi, L.K. Research on Ultra-High Strength Al-11Zn-2.9Mg-1.7Cu Alloy Prepared by Spray Forming Process. *Mater. Sci. Forum* **2005**, *475–479*, 2785–2788. [[CrossRef](#)]
44. Cai, Y.H.; Cui, H.; Li, Y.B.; Hang, J.F.; Zhang, J.S. Microstructure and Properties of Al-Zn-Mg-Cu-Mn in Situ High Strength Alloy. *Mater. Sci. Forum* **2007**, *561–565*, 957–960. [[CrossRef](#)]
45. Lu, Z.P.; Jiang, Y.Z.; Yu, L.H.; Xu, J.H.; Peng, J.D.; Xiang, K.Y. The Effect of Minor Scandium Addition on Microstructure Evolution and Mechanical Properties of Spray Formed Al-Zn-Mg-Cu Alloy. *J. Alloys Compd.* **2023**, *948*, 169710. [[CrossRef](#)]
46. Fan, C.; Li, Y.; Wu, Q.; Yang, J.; Hu, Z.; Ni, Y.; Ding, L. Effect of Cold Rolling Deformation on the Microstructure and Mechanical Properties of Spray-Formed Al-Zn-Mg-Cu Alloy. *J. Mater. Res.* **2024**, *39*, 471–479. [[CrossRef](#)]
47. Liu, C.Y.; Teng, G.B.; Ma, Z.Y.; Wei, L.L.; Zhou, W.B.; Huang, H.F.; Qi, H.Q. Mechanical Properties and Thermal Stability of 7055 Al Alloy by Minor Sc Addition. *Rare Met.* **2020**, *39*, 725–732. [[CrossRef](#)]
48. Zhang, G.W.; Feng, X.H.; Yang, Y.S. Effect of Minor Sc Addition on Microstructure and Tensile Properties of Hot-Extruded 7055 Alloy. *J. Mater. Eng. Perform.* **2022**, *31*, 6451–6458. [[CrossRef](#)]
49. Dong, P.X.; Chen, S.Y.; Chen, K.H. Effects of Cu Content on Microstructure and Properties of Super-High-Strength Al-9.3Zn-2.4Mg-XCu-Zr Alloy. *J. Alloys Compd.* **2019**, *788*, 329–337. [[CrossRef](#)]
50. Zou, Y.; Wu, X.D.; Tang, S.B.; Zhu, Q.Q.; Song, H.; Guo, M.X.; Cao, L.F. Investigation on Microstructure and Mechanical Properties of Al-Zn-Mg-Cu Alloys with Various Zn/Mg Ratios. *J. Mater. Sci. Technol.* **2021**, *85*, 106–117. [[CrossRef](#)]
51. Cai, W.D.; Lavernia, E.J. Modeling of Porosity During Spray Forming: Part I. Effects of Processing Parameters. *Metall. Mater. Trans. B* **1998**, *29*, 1085–1096. [[CrossRef](#)]
52. Xiang, X.; Zhang, Q.; Jiang, H.X.; Liu, C.; Cao, L.F. Micro Porosity and Its Effect on Fatigue Performance of 7050 Aluminum Thick Plates. *J. Cent. South Univ.* **2022**, *29*, 912–923.
53. Sanmarchi, C.; Liu, H.; Lavernia, E.J.; Rangel, R.H.; Sickinger, A.; Muehlberger, E. Numerical Analysis of the Deformation and Solidification of a Single Droplet Impinging onto a Flat Substrate. *J. Mater. Sci.* **1993**, *28*, 3313–3321.
54. Madejski, J. Solidification of Droplets on a Cold Surface. *Int. J. Heat Mass Transf.* **1976**, *19*, 1009–1013. [[CrossRef](#)]
55. Jia, Z.H.; Xie, Z.Q.; Xiang, K.Y.; Ding, L.P.; Weng, Y.Y.; Liu, Q. Effect of Heat Treatment and Extrusion Processing on the Microstructure and Mechanical Properties of Spray Formed 7055 Alloy. *Mater. Charact.* **2022**, *183*, 111619. [[CrossRef](#)]
56. Schreiber, J.M.; Omcikus, Z.R.; Eden, T.J.; Sharma, M.M.; Champagne, V.; Patankar, S.N. Combined Effect of Hot Extrusion and Heat Treatment on the Mechanical Behavior of 7055 AA Processed Via Spray Metal Forming. *J. Alloys Compd.* **2014**, *617*, 135–139. [[CrossRef](#)]
57. Khan, M.A.; Yang, W.W.; Afifi, M.A.; Malik, A.; Nazeer, F.; Yasin, G.; Jia, W.B.; Zhang, H. Microstructure and Mechanical Properties of an Al-Zn-Cu-Mg Alloy Processed by Hot Forming Processes Followed by Heat Treatments. *Mater. Charact.* **2019**, *157*, 109901. [[CrossRef](#)]
58. Zhao, W.J.; Cao, F.Y.; Gu, X.L.; Ning, Z.L.; Han, Y.; Sun, J.F. Isothermal Deformation of Spray Formed Al-Zn-Mg-Cu Alloy. *Mech. Mater.* **2013**, *56*, 95–105. [[CrossRef](#)]
59. Ning, Z.L.; Guo, S.; Zhang, M.X.; Cao, F.Y.; Jia, Y.D.; Sun, J.F. Characterization of the Secondary Phases in Spray Formed Al-Zn-Mg-Cu-Sc-Zr Alloy During Hot Compression. *J. Mater. Res.* **2016**, *16*, 2465–2472. [[CrossRef](#)]
60. Shao, Y.; Shi, J.H.; Pan, J.C.; Liu, Q.H.; Yan, L.; Guo, P.Y. Influence of Thermo-Mechanical Conditions on the Microstructure and Mechanical Property of Spray-Formed 7055 Aluminum Alloy. *Mater. Today Commun.* **2022**, *31*, 103593. [[CrossRef](#)]
61. Robinson, J.S.; Cudd, R.L.; Tanner, D.A.; Dolan, G.P. Quench Sensitivity and Tensile Property Inhomogeneity in 7010 Forgings. *J. Mater. Process. Technol.* **2001**, *119*, 261–267. [[CrossRef](#)]
62. Godinho, H.A.; Beletati, A.L.R.; Giordano, E.J.; Claudemiro, B. Microstructure and Mechanical Properties of a Spray Formed and Extruded Aa7050 Recycled Alloy. *J. Alloys Compd.* **2014**, *586*, S139–S142. [[CrossRef](#)]
63. Yuan, C.P.; Bai, P.C.; Zhang, X.Y.; Zhang, H.J.; Guo, S.L. Researches of Structures and Mechanical Properties of Spray Formed Al-Zn-Mg-Cu Alloy. *Rare Met. Mater. Eng.* **2007**, *36*, 480–483.

64. Tian, D.Y.; Wang, R.; Zheng, J. Research on the Mechanical Properties and Hot Deformation Behaviors of Spray-Deposited 7034 Al Alloy Processed by Forward Extrusion. *J. Mater. Eng. Perform.* **2022**, *31*, 37–52. [[CrossRef](#)]
65. Wang, X.D.; Pan, Q.L.; Liu, L.L.; Xiong, S.W.; Wang, W.Y.; Lai, J.P.; Sun, Y.W.; Huang, Z.Q. Characterization of Hot Extrusion and Heat Treatment on Mechanical Properties in a Spray Formed Ultra-High Strength Al-Zn-Mg-Cu Alloy. *Mater. Charact.* **2018**, *144*, 131–140. [[CrossRef](#)]
66. Wei, Q.; Xiong, B.Q.; Zhang, Y.N.; Zhu, B.H.; Shi, L.K. Production of High Strength Al-Zn-Mg-Cu Alloys by Spray Forming Process. *Trans. Nonferrous Met. Soc. China* **2001**, *11*, 258–261.
67. Kishchik, A.A.; Kishchik, M.S.; Kotov, A.D.; Mikhaylovskaya, A.V. Effect of Multidirectional Forging on the Microstructure and Mechanical Properties of the Al-Mg-Mn-Cr Alloy. *Phys. Met. Metallogr.* **2020**, *121*, 489–494. [[CrossRef](#)]
68. Xu, C.T.; Xu, B.; Shi, W.C.; Xue, K.M. Experimental Study on Densification of Spray-Formed High-Strength Aluminum Alloy by Square Cladding Forging. *Int. J. Plast.* **2021**, *28*, 136–142.
69. Liu, T.; Jiang, H.T.; Sun, H.; Wang, Y.J.; Dong, Q.; Zeng, J.R.; Bian, F.G.; Zhang, J.; Chen, F.; Sun, B.D. Effects of Rolling Deformation on Precipitation Behavior and Mechanical Properties of Al-Zn-Mg-Cu Alloy. *Mater. Sci. Eng. A* **2022**, *847*, 143342. [[CrossRef](#)]
70. Zhang, T.; Wu, Y.X.; Gong, H.; Zheng, X.Z.; Jiang, S.S. Effects of Rolling Parameters of Snake Hot Rolling on Strain Distribution of Aluminum Alloy 7075. *Trans. Nonferrous Met. Soc. China* **2014**, *24*, 2150–2156. [[CrossRef](#)]
71. Zhang, T.; Li, L.; Lu, S.H.; Zhang, J.B.; Gong, H. Comparisons of Flow Behavior Characteristics and Microstructure between Asymmetrical Shear Rolling and Symmetrical Rolling by Macro/Micro Coupling Simulation. *J. Comput. Sci.* **2018**, *29*, 142–152. [[CrossRef](#)]
72. Su, H.; Hou, L.G.; Tian, Q.k.; Wang, Y.W.; Zhuang, L.Z. Understanding the Bending Behavior and through-Thickness Strain Distribution During Asymmetrical Rolling of High-Strength Aluminium Alloy Plates. *J. Mater. Res. Technol.* **2023**, *22*, 1462–1475. [[CrossRef](#)]
73. Mei, L.; Chen, X.P.; Ren, P.; Nie, Y.Y.; Huang, G.J.; Liu, Q. Effect of Warm Deformation on Precipitation and Mechanical Properties of a Cryorolled Al-Zn-Mg-Cu Sheet. *Mater. Sci. Eng. A* **2020**, *771*, 138608. [[CrossRef](#)]
74. Wang, F.; Xiong, B.Q.; Zhang, Y.G.; Liu, H.W.; Li, Z.H.; Liu, Q. Microstructure and Mechanical Properties of Spray-Deposited Al-Zn-Mg-Cu Alloy Processed through Hot Rolling and Heat Treatment. *Mater. Sci. Eng. A* **2009**, *518*, 144–149. [[CrossRef](#)]
75. Lang, H.J.; Wu, X.J.; Hong, B.; Teng, J.Z.; Huang, S.Q.; Miao, J. Dislocation Density Model and Microstructure of 7A85 Aluminum Alloy During Thermal Deformation. *J. Cent. South Univ.* **2021**, *28*, 2999–3007.
76. Lin, X.M.; Wu, X.D.; Cao, L.F.; Tang, S.B.; Bai, M. Effect of Hot Deformation on the Microstructure of Spray-Formed 7055 Aluminum Alloy Extruded Plate. *J. Cent. South Univ.* **2023**, *30*, 3950–3963. [[CrossRef](#)]
77. Lin, X.M.; Wu, X.D.; Cao, L.F.; Tang, S.B.; He, B.S. The Effects of Heat Treatment on the Extrusion-Induced Inhomogeneity of Spray-Formed Aluminum Alloy 7055. *J. Mater. Res. Technol.-JMRT* **2023**, *25*, 2075–2087. [[CrossRef](#)]
78. Aryshenskii, E.; Jürgen, H.; Vasilii, Y.; Konovalov, S.; Rudolf, K. Influence of Local Inhomogeneity of Thermomechanical Treatment Conditions on Microstructure Evolution in Aluminum Alloys. *J. Mater. Eng. Perform.* **2018**, *27*, 6780–6799. [[CrossRef](#)]
79. Zhang, X.M.; Han, N.M.; Liu, S.D.; Song, F.X.; Zeng, R.L.; Huang, L.Y. Inhomogeneity of Texture, Tensile Property and Fracture Toughness of 7050 Aluminum Alloy Thick Plate. *Trans. Nonferrous Met. Soc. China* **2010**, *20*, 202–208.
80. She, H.; Shu, D.; Wang, J.; Sun, B.D. Influence of Multi-Microstructural Alterations on Tensile Property Inhomogeneity of 7055 Aluminum Alloy Medium Thick Plate. *Mater. Charact.* **2016**, *113*, 189–197. [[CrossRef](#)]
81. Kim, J.H.; Kim, J.H.; Yeom, J.T.; Lee, D.G.; Lim, S.G.; Park, N.K. Effect of Scandium Content on the Hot Extrusion of Al-Zn-Mg-(Sc) Alloy. *J. Mater. Process. Technol.* **2007**, *187–188*, 635–639. [[CrossRef](#)]
82. Van Geertruyden, W.H.; Browne, H.M.; Misiolek, W.Z.; Wang, P.T. Evolution of Surface Recrystallization During Indirect Extrusion of 6xxx Aluminum Alloys. *Metall. Mater. Trans. A* **2005**, *36A*, 1049–1056. [[CrossRef](#)]
83. Sun, S.Q.; Fang, Y.; Zhang, L.; Li, C.L.; Hu, S.Q. Effects of Aging Treatment and Peripheral Coarse Grain on the Exfoliation Corrosion Behaviour of 2024 Aluminium Alloy Using Sr-Ct. *J. Mater. Res. Technol.* **2020**, *9*, 3219–3229. [[CrossRef](#)]
84. Li, P.; Wang, S.; Dong, H.G.; Wen, G.D.; Yu, F.Y.; Ma, Y.T.; Lei, Z.K. Effect of Inhomogeneous Microstructure Evolution on the Mechanical Properties and Corrosion Behavior of Rotary Friction Welded AA2024 Joints. *Mater. Charact.* **2021**, *178*, 111306. [[CrossRef](#)]
85. Zhao, N.; Ma, H.J.; Sun, Q.; Hu, Z.L.; Yan, Y.; Chen, T.F.; Hua, L. Microstructural Evolutions and Mechanical Properties of 6082 Aluminum Alloy Part Produced by a Solution-Forging Integrated Process. *J. Mater. Process. Technol.* **2022**, *308*, 117715. [[CrossRef](#)]
86. Feng, C.; Shou, W.B.; Liu, H.Q.; Yi, D.Q.; Feng, Y.R. Microstructure and Mechanical Properties of High Strength Al-Zn-Mg-Cu Alloys Used for Oil Drill Pipes. *Trans. Nonferrous Met. Soc. China* **2015**, *25*, 3515–3522. [[CrossRef](#)]
87. Xu, D.K.; Birbilis, N.; Lashansky, D.; Rometsch, P.A.; Muddle, B.C. Effect of Solution Treatment on the Corrosion Behaviour of Aluminium Alloy AA7150: Optimisation for Corrosion Resistance. *Corros. Sci.* **2011**, *53*, 217–225. [[CrossRef](#)]
88. Wu, H.; Wen, S.P.; Huang, H.B.; Li, L.; Wu, X.L.; Gao, K.Y.; Wang, W.; Nie, Z.R. Effects of Homogenization on Precipitation of Al₃(Er,Zr) Particles and Recrystallization Behavior in a New Type Al-Zn-Mg-Er-Zr Alloy. *Mater. Sci. Eng. A* **2017**, *689*, 313–322. [[CrossRef](#)]
89. Wu, C.H.; Feng, D.; Ren, J.J.; Zang, Q.H.; Li, J.C.; Liu, S.D.; Zhang, X.M. Effect of Non-Isothermal Retrogression and Re-Ageing on through-Thickness Homogeneity of Microstructure and Properties of Al-8Zn-2Mg-2Cu Alloy Thick Plate. *J. Cent. South Univ.* **2022**, *29*, 960–972. [[CrossRef](#)]

90. Wang, Z.P.; Geng, J.W.; Pu, Q.Q.; Li, K.N.; Luo, T.; Li, Y.G.; Xia, P.K.; Li, X.F.; Chen, D.; Sha, G.; et al. Achieving High Performance by Optimized Heat Treatment in a Spray Formed Al-Zn-Mg-Cu Alloy. *Mater. Sci. Eng. A* **2024**, *893*, 146134. [[CrossRef](#)]
91. Wang, X.D.; Pan, Q.L.; Wang, W.Y.; Huang, Z.Q.; Chen, J.; Pan, B.Q.; Liu, X. Effects of Pre-Strain and Aging Treatments on the Mechanical Property and Corrosion Resistance of the Spray Formed Ultra-High Strength Al-Zn-Mg-Cu Alloy. *Mater. Charact.* **2022**, *194*, 112381. [[CrossRef](#)]
92. Guo, S.; Zhi, L.; Ning, L.; Cao, F.Y.; Sun, J.F. Microstructural Evolution of Spray-Formed Al-11.5Zn-2.0Mg-1.6Cu Alloy During Hot-Extrusion and Heat-Treatment. *Trans. Nonferrous Met. Soc. China* **2009**, *19*, 343–348. [[CrossRef](#)]
93. Wang, F.; Xiong, B.Q.; Zhang, Y.G.; Liu, H.W.; He, X.Q. Microstructural Development of Spray-Deposited Al-Zn-Mg-Cu Alloy During Subsequent Processing. *J. Alloys Compd.* **2009**, *477*, 616–621. [[CrossRef](#)]
94. Yu, H.C.; Wang, M.P.; Sheng, X.F.; Li, Z.; Chen, L.B.; Lei, Q.; Chen, C.; Jia, Y.L.; Xiao, Z.; Chen, W.; et al. Microstructure and Tensile Properties of Large-Size 7055 Aluminum Billets Fabricated by Spray Forming Rapid Solidification Technology. *J. Alloys Compd.* **2013**, *578*, 208–214. [[CrossRef](#)]
95. Shen, G.W.; Chen, X.L.; Yan, J.; Fan, L.Y.; Yang, Z.; Zhang, J.; Guan, R.G. Effects of Heat Treatment Processes on the Mechanical Properties, Microstructure Evolution, and Strengthening Mechanisms of Al-Mg-Zn-Cu Alloy. *J. Mater. Res. Technol.* **2023**, *27*, 5380–5388. [[CrossRef](#)]
96. Liu, S.D.; Li, C.B.; Han, S.Q.; Deng, Y.L.; Zhang, X.M. Effect of Natural Aging on Quench-Induced Inhomogeneity of Microstructure and Hardness in High Strength 7055 Aluminum Alloy. *J. Alloys Compd.* **2015**, *625*, 34–43. [[CrossRef](#)]
97. Sharma, M.M.; Amateau, M.F.; Eden, T.J. Mesoscopic Structure Control of Spray Formed High Strength Al-Zn-Mg-Cu Alloys. *Acta Mater.* **2005**, *10*, 2919–2924. [[CrossRef](#)]
98. Cheng, Y.; Xu, J.H.; Yu, L.H.; Hu, Y.X.; Huang, T.; Zhang, H. Effect of Non-Isothermal Aging Treatments on the Microstructure and Properties of Tic-Tib₂ Ceramic Particles-Reinforced Spray-Formed 7055 Aluminum Alloy Tig Weld Metal. *J. Mater. Sci.* **2023**, *45*, 17241–17256. [[CrossRef](#)]
99. Guo, G.; Jiang, J.; Li, W.; Li, C.Y. Effects of Aging Treatment on Nano-Sized Precipitates and Properties of Spray Formed Al-Zn-Mg-Cu Alloy. *Nanosci. Nanotechnol. Lett.* **2018**, *10*, 112–118.
100. Ditta, A.; Wei, L.J.; Xu, Y.J.; Wu, S.J. Microstructural Characteristics and Properties of Spray Formed Zn-Rich Al-Zn-Mg-Cu Alloy under Various Aging Conditions. *Mater. Charact.* **2020**, *161*, 110133. [[CrossRef](#)]
101. Sharma, M.M.; Amateau, M.F.; Eden, T.J. Aging Response of Al-Zn-Mg-Cu Spray Formed Alloys and Their Metal Matrix Composites. *Mater. Sci. Eng. A* **2006**, *1*, 87–96. [[CrossRef](#)]
102. Guo, G.; Zhang, L.Y.; Yuan, H.J.; Jiang, J.B.; Ouyang, M.; Xu, L.J. Second Step Aging on Nanosized Precipitates and Properties of Al-Zn-Mg-Cu-Cr Spray-Deposited Alloys. *J. Nanosci. Nanotechnol.* **2020**, *3*, 1955–1961.
103. Su, R.M.; Qu, Y.D.; You, J.H.; Li, R.D. Study on a New Retrogression and Re-Aging Treatment of Spray Formed Al-Zn-Mg-Cu Alloy. *J. Mater. Res.* **2016**, *5*, 573–579. [[CrossRef](#)]
104. He, X.; Xiong, B.; Sun, Z.; Zhang, Y.C.; Wang, F.; Zhu, B. Microstructural Evolution of the Spray Formed Al-Zn-Mg-Cu Alloy During Extrusion and Heat Treatment. *Rare Metal Mater. Eng.* **2008**, *37*, 534–537.
105. Wang, Z.P.; Geng, J.W.; Xia, P.K.; Li, Y.G.; Chen, W.; Li, X.F.; Wang, M.L.; Chen, D.; Wang, H.W. Phase Transformation from H Phase to S Phase at Grain Boundary During Annealing in Rapidly-Solidified Al-Zn-Mg-Cu Alloy. *Mater. Charact.* **2023**, *195*, 112531. [[CrossRef](#)]
106. Khan, M.A.; Wang, Y.W.; Yasin, G.; Nazeer, F.; Malik, A.; Khan, W.Q.; Ahmad, T.; Zhang, H.; Afifi, M.A. The Effect of Strain Rates on the Microstructure and the Mechanical Properties of an over-Aged Al-Zn-Mg-Cu Alloy. *Mater. Charact.* **2020**, *167*, 110472. [[CrossRef](#)]
107. Chung, T.F.; Yang, Y.L.; Shiojiri, M.; Hsiao, C.N.; Li, W.C.; Tsao, C.S.; Shi, Z.S.; Lin, J.G.; Yang, J.R. An Atomic Scale Structural Investigation of Nanometre-Sized H precipitates in the 7050 Aluminium Alloy. *Acta Mater.* **2019**, *174*, 351–368. [[CrossRef](#)]
108. Chung, T.F.; Yang, Y.L.; Huang, B.M.; Shi, Z.S.; Lin, J.G.; Ohmura, T.; Yang, J.R. Transmission Electron Microscopy Investigation of Separated Nucleation and in-Situ Nucleation in AA7050 Aluminium Alloy. *Acta Mater.* **2018**, *149*, 377–387. [[CrossRef](#)]
109. Mazzer, E.M.; Afonso, C.R.M.; Galano, M.; Kiminami, C.S.; Bolfarini, C. Microstructure Evolution and Mechanical Properties of Al-Zn-Mg-Cu Alloy Reprocessed by Spray-Forming and Heat Treated at Peak Aged Condition. *J. Alloys Compd.* **2013**, *579*, 169–173. [[CrossRef](#)]
110. Wang, H.; Chen, M.; Liu, H.; Huang, J.; Yang, B.; Zhang, J. Experimental Investigation on Heat Treatment of Spray-Forming Ultrahigh Strength Al-Zn-Mg-Cu Alloys. *J. Univ. Sci. Technol. Beijing* **2003**, *25*, 436–440.
111. Peng, X.Y.; Li, Y.; Liang, X.P. Precipitate Behavior and Mechanical Properties of Enhanced Solution Treated Al-Zn-Mg-Cu Alloy During Non-Isothermal Ageing. *J. Alloys Compd.* **2018**, *735*, 964–974. [[CrossRef](#)]
112. Feng, D.; Xu, R.; Li, J.C.; Huang, W.J.; Wang, J.T.; Liu, Y.; Zhao, L.X.; Li, C.B.; Zhang, H. Microstructure Evolution Behavior of Spray-Deposited 7055 Aluminum Alloy During Hot Deformation. *Metals* **2022**, *12*, 1982. [[CrossRef](#)]
113. Guo, S.; Ning, Z.L.; Cao, F.Y.; Sun, J.F. Secondary Phases Present in Spray Formed Al-10.5Zn-2.0Mg-1.5Cu Alloy. *Adv. Mater. Res.* **2010**, *97–101*, 1073–1076. [[CrossRef](#)]
114. Si, C.R.; Tang, X.L.; Zhang, X.L.; Wang, J.B.; Wu, W.C. Microstructure and Mechanical Properties of Low-Pressure Spray-Formed Zn-Rich Aluminum Alloy. *Mater. Express* **2017**, *7*, 273–282. [[CrossRef](#)]

115. Yang, Y.G.; Zhao, Y.T.; Kai, X.Z.; Zhang, Z.; Zhang, H.; Tao, R.; Chen, G.; Yin, H.S.; Wang, M. Effects of Hot Extrusion and Heat Treatment on Microstructure and Properties of Industrial Large-Scale Spray-Deposited 7055 Aluminum Alloy. *Mater. Res. Express* **2018**, *5*, 016519. [[CrossRef](#)]
116. He, B.S.; Cao, L.F.; Wu, X.D.; Tang, S.B.; Lin, X.M.; Zou, Y. Effect of Continuous Retrogression and Re-Ageing Treatment on Mechanical Properties, Corrosion Behavior and Microstructure of an Al-Zn-Mg-Cu Alloy. *J. Alloys Compd.* **2023**, *970*, 172592. [[CrossRef](#)]
117. Xu, X.S.; Zheng, J.X.; Li, Z.; Luo, R.C.; Chen, B. Precipitation in an Al-Zn-Mg-Cu Alloy During Isothermal Aging: Atomic-Scale Haadf-Stem Investigation. *Mater. Sci. Eng. A* **2017**, *691*, 60–70. [[CrossRef](#)]
118. Sha, G.; Cerezo, A. Early-Stage Precipitation in Al-Zn-Mg-Cu Alloy (7050). *Acta Mater.* **2004**, *52*, 4503–4516. [[CrossRef](#)]
119. Hou, X.H.; Bai, P.C.; Zhang, X.Y.; Dong, T.S.; Cui, X.M.; Wang, N. Analysis for Precipitates of Spray Formed Al-Zn-Mg-Cu Alloy after Aging. *Rare Met. Mater. Eng.* **2010**, *39*, 332–335.
120. Lin, X.M.; Cao, L.F.; Wu, X.D.; Tang, S.B.; Zou, Y. Precipitation Behavior of Spray-Formed Aluminum Alloy 7055 During High Temperature Aging. *Mater. Charact.* **2022**, *194*, 112347. [[CrossRef](#)]
121. Zou, Y.; Wu, X.D.; Tang, S.B.; Zhu, Q.Q.; Cao, L.F. Co-Precipitation of T' and H' Phase in Al-Zn-Mg-Cu Alloys. *Mater. Charact.* **2020**, *169*, 110610. [[CrossRef](#)]
122. Hou, S.L.; Zhang, D.; Ding, Q.W.; Zhang, J.S.; Zhuang, L.Z. Solute Clustering and Precipitation of Al-5.1Mg-0.15Cu-XZn Alloy. *Mater. Sci. Eng. A* **2019**, *759*, 465–478. [[CrossRef](#)]
123. Ma, K.; Wen, H.; Hu, T.; Topping, T.D.; Isheim, D.; Seidman, D.N.; Lavernia, E.J.; Schoenung, J.M. Mechanical behavior and strengthening mechanisms in ultrafine grain precipitation-strengthened aluminum alloy. *Acta Mater.* **2014**, *62*, 141–155. [[CrossRef](#)]
124. Liao, H.C.; Li, G.J.; Liu, Q. Ni-Rich Phases in Al-12%Si-4%Cu-1.2%Mn-X%Ni Heat-Resistant Alloys and Effect of Ni-Alloying on Tensile Mechanical Properties. *J. Mater. Eng. Perform.* **2019**, *28*, 5398–5408. [[CrossRef](#)]
125. Tan, P.; Sui, Y.D.; Jin, H.N.; Zhu, S.; Jiang, Y.H.; Han, L.N. Effect of Zn Content on the Microstructure and Mechanical Properties of as-Cast Al-Zn-Mg-Cu Alloy with Medium Zn Content. *J. Mater. Res. Technol.* **2022**, *18*, 2620–2630. [[CrossRef](#)]
126. Salamci, E. Ageing Behaviour of Spray Cast Al-Zn-Mg-Cu Alloys. *Turk. J. Eng. Env. Sci. E* **2001**, *25*, 681–686.
127. Chen, Z.Y.; Yuan, K.M.; Nie, Z.R. Effect of Zn Content on the Microstructure and Properties of Super-High Strength Al-Zn-Mg-Cu Alloys. *Metall. Mater. Trans. A* **2013**, *44*, 3910–3920. [[CrossRef](#)]
128. Shu, W.X.; Hou, L.G.; Zhang, C.; Zhang, F.; Liu, J.C.; Liu, J.T.; Zhuang, L.Z.; Zhang, J.S. Tailored Mg and Cu Contents Affecting the Microstructures and Mechanical Properties of High-Strength Al-Zn-Mg-Cu Alloys. *Mater. Sci. Eng. A* **2016**, *657*, 269–283. [[CrossRef](#)]
129. Guo, Z.Y.; Zhao, G.; Chen, X.G. Effects of Two-Step Homogenization on Precipitation Behavior of Al₃Zr Dispersoids and Recrystallization Resistance in 7150 Aluminum Alloy. *Mater. Charact.* **2015**, *102*, 122–130. [[CrossRef](#)]
130. Zhang, M.; Liu, T.; He, C.N.; Ding, J.; Liu, E.Z.; Shi, C.S.; Li, J.J.; Zhao, N.Q. Evolution of Microstructure and Properties of Al-Zn-Mg-Cu-Sc-Zr Alloy During Aging Treatment. *J. Alloys Compd.* **2016**, *68*, 946–951. [[CrossRef](#)]
131. Deng, Y.; Zhi, M.Y.; Zhao, K.; Duan, J.Q.; Hu, J.; He, Z.B. Effects of Sc and Zr Microalloying Additions and Aging Time at 120 °C on the Corrosion Behaviour of an Al-Zn-Mg Alloy. *Corros. Sci.* **2012**, *65*, 288–298. [[CrossRef](#)]
132. Sharma, M.M.; Amateau, M.F.; Eden, T.J. Hardening Mechanisms of Spray Formed Al-Zn-Mg-Cu Alloys with Scandium and Other Elemental Additions. *J. Alloys Compd.* **2006**, *416*, 135–142. [[CrossRef](#)]
133. Li, Z.L.; Xie, J.X.; Chen, W.; Zhai, J.; Ren, H.P.; Wang, Y.F. Structure and Property of Nickel-Modified Ultrahigh Strength Al-Zn-Mg-Cu Alloy by Spray Forming. *Mater. Sci. Forum* **2007**, *546–549*, 871–876. [[CrossRef](#)]
134. Tsivoulas, D.; Robson, J.D. Heterogeneous Zr Solute Segregation and Al₃Zr Dispersoid Distributions in Al-Cu-Li Alloys. *Acta Mater.* **2015**, *93*, 73–86. [[CrossRef](#)]
135. Zhang, Z.W.; Liu, R.X.; Li, D.Y.; Peng, Y.H.; Zhou, G.W.; Jia, Z.H.; Ma, W.T. Investigation on Deformation Behaviors and Dynamic Recrystallization Mechanism of Spray Formed Al-Zn-Mg-Cu Alloy under Hot Compression. *J. Mater. Res. Technol.* **2024**, *28*, 4401–4416. [[CrossRef](#)]
136. Wang, Z.P.; Xiao, H.Y.; Chen, W.; Li, Y.G.; Geng, J.W.; Li, X.F.; Xia, P.K.; Wang, M.L.; Chen, D.; Wang, H.W. New Insight into Precipitation of Al₃Zr and Correlative Effect on Recrystallization Behavior in a Rapidly-Solidified Al-Zn-Mg-Cu-Zr Alloy. *Mater. Charact.* **2022**, *191*, 112142. [[CrossRef](#)]
137. Kang, Y.C.; Chan, S.L.I. Tensile Properties of Nanometric Al₂O₃ Particulate-Reinforced Aluminum Matrix Composites. *Mater. Chem. Phys.* **2004**, *85*, 438–443. [[CrossRef](#)]
138. Rohrer, G.S. "Introduction to Grains, Phases, and Interfaces—An Interpretation of Microstructure," *Trans. AIME*, 1948, vol. 175, pp. 15–51, by C.S. Smith. *Metall. Mater. Trans. B-Proc. Metall. Mater. Proc. Sci.* **2010**, *41*, 457–494. [[CrossRef](#)]
139. Nes, E. Recrystallization and Texture Control During Process. In *Proceedings of the Aluminium Technology'86*, the Royal Lancaster Hotel, London, UK, 11–13 March 1986.
140. Nes, E.; Ryum, N.; Hunderi, O. On the Zener Drag. *Acta Metall. Mater.* **1985**, *33*, 11–12. [[CrossRef](#)]
141. She, H.; Shu, D.; Dong, A.P.; Wang, J.; Sun, B.D.; Lai, H.C. Relationship of Particle Stimulated Nucleation, Recrystallization and Mechanical Properties Responding to Fe and Si Contents in Hot-Extruded 7055 Aluminum Alloys. *J. Mater. Sci. Technol.* **2019**, *35*, 2570–2581. [[CrossRef](#)]
142. Hall, E.O. The Deformation and Ageing of Mild Steel: III Discussion of Results. *Proc. Phys. Soc. Sect. B* **1951**, *64*, 747–753. [[CrossRef](#)]

143. Petch, N.J. The Cleavage Strength of Polycrystals. *J. Iron Steel Inst.* **1953**, *174*, 25–28.
144. Wen, K.; Xiong, B.Q.; Zhang, Y.A.; Wang, G.J.; Li, X.W.; Li, Z.H.; Huang, S.H.; Liu, H.W. Microstructure Evolution of a High Zinc Containing Al-Zn-Mg-Cu Alloy During Homogenization. *Rare Met. Mater. Eng.* **2017**, *46*, 928–934.
145. Li, H.Y.; Liu, J.J.; Yu, W.C.; Zhao, H.; Li, D.W. Microstructure Evolution of Al-Zn-Mg-Cu Alloy During Non-Linear Cooling Process. *Trans. Nonferrous Met. Soc. China* **2016**, *26*, 1191–1200. [[CrossRef](#)]
146. Polmear, I.J.; Couper, M.J. Design and Development of an Experimental Wrought Aluminum-Alloy for Use at Elevated-Temperatures. *Metall. Mater. Trans. A* **1998**, *19*, 1027–1035. [[CrossRef](#)]
147. Rong, H.; Hu, P.; Ying, L.; Hou, W.B.; Zhang, J.H. Thermal Forming Limit Diagram (Tfld) of AA7075 Aluminum Alloy Based on a Modified Continuum Damage Model: Experimental and Theoretical Investigations. *Int. J. Mech. Sci.* **2019**, *156*, 59–73. [[CrossRef](#)]
148. Guo, Y.; Zhou, M.X.; Sun, X.D.; Qian, L.; Li, L.J.; Xie, Y.J.; Liu, Z.Y.; Wu, D.; Yang, L.G.; Wu, T.; et al. Effects of Temperature and Strain Rate on the Fracture Behaviors of an Al-Zn-Mg-Cu Alloy. *Materials* **2018**, *11*, 1233. [[CrossRef](#)] [[PubMed](#)]
149. Jiang, F.L.; Zhang, H.; Su, J.; Sun, Y.S. Constitutive Characteristics and Microstructure Evolution of 7150 Aluminum Alloy During Isothermal and Non-Isothermal Multistage Hot Compression. *Mater. Sci. Eng. A* **2015**, *636*, 459–469. [[CrossRef](#)]
150. Dai, P.; Luo, X.; Yang, Y.Q.; Kou, Z.D.; Huang, B.; Zang, J.X.; Ru, J.G. High Temperature Tensile Properties, Fracture Behaviors and Nanoscale Precipitate Variation of an Al-Zn-Mg-Cu Alloy. *Prog. Nat. Sci.* **2020**, *30*, 63–73. [[CrossRef](#)]
151. Elagin, V.I. Ways of Developing High-Strength and High-Temperature Structural Aluminum Alloys in the 21st Century. *Met. Sci. Heat Treat.* **2007**, *49*, 427–434. [[CrossRef](#)]
152. Lang, M.; Zhao, N.; Wang, Y.C.; He, M.; Zhu, J.; Qiao, J. Effect of Minor Sc Addition on High Temperature Tensile Behavior of Al-7Zn-2Mg-2Cu-0.2Zr Alloy. *Mater. Chem. Phys.* **2022**, *288*, 126334. [[CrossRef](#)]
153. Zhai, F.L.; Wang, L.P.; Gao, X.S.; Zhao, C.; Feng, Y.C.; Ma, T.; Fan, R. Effect of Samarium on the High Temperature Tensile Properties and Fracture Behaviors of Al-Zn-Mg-Cu-Zr Alloy. *Mater. Res.* **2021**, *8*, 016521. [[CrossRef](#)]
154. Han, W.H.; Li, Y.; Li, P.; Su, G.P.; Zhang, C.Z.; Sun, C.F.; Chen, C.G.; Yang, F.; Guo, Z.M. Microstructure and Mechanical Properties at Elevated Temperature of Powder Metallurgy Al-Zn-Mg-Cu Alloy Subjected to Hot Extrusion. *Metals* **2022**, *12*, 259. [[CrossRef](#)]
155. Wang, Y.X.; Wu, G.H.; Zhang, L.; Guo, Y.J.; Wang, C.L.; Li, L.B.; Xiong, X.M. Microstructure Evolution and Mechanical Properties of a Cast and Heat-Treated Al-Li-Cu-Mg Alloy: Effect of Cooling Rate During Casting. *Mater. Sci. Eng. A* **2023**, *880*, 145366. [[CrossRef](#)]
156. Zare, M.A.; Taghiabadi, R.; Ghoncheh, M.H. Effect of Cooling Rate on Microstructure and Mechanical Properties of AA5056 Al-Mg Alloy. *Int. J. Met.* **2022**, *16*, 1533–1543. [[CrossRef](#)]
157. Yang, Q.B.; Shi, W.J.; Wang, M.; Jia, L.; Wang, W.B.; Zhang, H. Influence of Cooling Rate on the Microstructure and Mechanical Properties of Al-Cu-Li-Mg-Zn Alloy. *J. Mater. Res. Technol.* **2023**, *25*, 3151–3166. [[CrossRef](#)]
158. Uzan, N.E.; Shneck, R.; Yeheskel, O.; Frage, N. High-Temperature Mechanical Properties of AlSi10Mg Specimens Fabricated by Additive Manufacturing Using Selective Laser Melting Technologies (Am-Slm). *Addit. Manuf.* **2018**, *24*, 257–263. [[CrossRef](#)]
159. Mattson, J.; Theisen, E.; Steen, P. Rapid Solidification Forming of Glassy and Crystalline Ribbons by Planar Flow Casting. *Chem. Eng. Sci.* **2018**, *192*, 1198–1208. [[CrossRef](#)]
160. Tournet, D.; Reinhart, G.; Gandin, C.A.; Iles, G.N.; Dahlborg, U.; Calvo-Dahlborg, M.; Bao, C.M. Gas Atomization of Al-Ni Powders: Solidification Modeling and Neutron Diffraction Analysis. *Acta Mater.* **2011**, *59*, 6658–6669. [[CrossRef](#)]
161. Liu, B.; Lei, Q.; Xie, L.Q.; Wang, M.P.; Li, Z. Microstructure and Mechanical Properties of High Product of Strength and Elongation Al-Zn-Mg-Cu-Zr Alloys Fabricated by Spray Deposition. *Mater. Des.* **2016**, *96*, 217–223. [[CrossRef](#)]
162. Wang, F.; Zhu, B.H.; Xiong, B.Q.; Zhang, Y.A.; Liu, H.W.; Zhang, R.H. An Investigation on the Microstructure and Mechanical Properties of Spray-Deposited Al-8.5Fe-1.1V-1.9Si Alloy. *J. Mater. Process. Technol.* **2007**, *183*, 386–389. [[CrossRef](#)]

Disclaimer/Publisher’s Note: The statements, opinions and data contained in all publications are solely those of the individual author(s) and contributor(s) and not of MDPI and/or the editor(s). MDPI and/or the editor(s) disclaim responsibility for any injury to people or property resulting from any ideas, methods, instructions or products referred to in the content.